Republic of Iraq
Ministry of Higher Education and Scientific Research
Al-Nahrain University
College of Science
Department of Computer

Satellite Image Classification Using K-Means and SVD Techniques

A Thesis

Submitted to the College of Science / Al-Nahrain University as a Partial Fulfillment of the requirements for the Degree of Master of Science in Computer Science

By

Assad Hussein Thary

B.Sc. in Computer Science / College of Science / Al-Nahrain University (2014)

Supervised by
Asst.Prof.Dr. Mohammed Sahib Altaei

Ramadan **1437 A. H.**

May **2016 A. D.**

قال الله تعالى

سورة يوسف/76

DEDICATED TO

My Parents
MY Brothers

To everyone
Taught me a letter

Acknowledgments

I would like to acknowledge my sincere thanks and appreciation to my supervisor Dr. Mohammed S. Altaei for suggesting the research, assistance, encouragement, valuable advice, for giving me the major steps to go on to explore the subject, sharing with me the ideas in my research "SATELLITE IMAGE CLASSIFICATION USING KMEANS and SVD TECHNIQUES ", and discuss the points that I left they are important.

Grateful Thanks are due to the Head of Computer Science Department, and the staff of the Department at College of Science of Al-Nahrain University for their kind attention.

Sincere thanks to my father for his efforts, and family for their help and patience, and thanks to my faithful friends for supporting and giving me advises.

Assad

2016

ABSTRACT

The use of remote sensing technologies was gained more attention due to an increasing need to collect data for the environmental dynamics. Digital image analysis has been used for forest mapping and inventory evaluations, and it has played a substantial role in landcover monitoring and assessment. Satellite image classification is a relatively recent type of remote sensing uses satellite imagery to indicate many key environment characteristics.

The motivation of current research is addressed at establishing a satellite image classification based on Singular Value Decomposition (SVD) technique. In addition to the preprocessing stages, the proposed classification method is designed to be consisted of two phases: enrollment and classification. It was intended for the proposed method to be used the SVD and applied on multispectral satellite image, the used image is pictured by Landsat satellite for Baghdad city in Iraq with medium resolution of 1024×1024*pixel*. The enrollment phase aims at extracting the image classes to be stored in dataset as a training data. Since the SVD method is supervised method, it cannot enroll the intended dataset, instead, the moment based K-means was used to build the dataset. Thereby, the enrollment phase began with partitioning the image into uniform sized blocks, and estimating the moment for each image block. The moment is the feature by which the image blocks were grouped. Then, K-means is used to cluster the image blocks and determining the number of cluster and centroid of each cluster. The image block corresponding to these centroids were stored in the dataset to be used in the classification phase.

The enrollment phase showed that the image contains five distinct classes: water, vegetation, residential without vegetation, residential with vegetation, and open land. Therefore, a specific image block of each class stored in dataset to be act as training area. These training areas pointed on the image and monitored to validate the available information of classes.

SVD based classification method required to be consisted of multi stages, these are: image composition, image transform, image partitioning, feature extraction, and then image classification. The image partitioning stage was carried out by quadtree method. The practice and analysis showed there were many effective conditions affect image partitioning, the analysis help to achieve the best values of such conditions to get best results. The proposed classification method used the dataset to estimate the classification feature of SVD and compute the similarity measure for each block in the image. The similarity measure indicates the

class of the dataset that the image block was belongs to. Frequently, the image is classified block by block and then the classified image is displayed.

After assurance the acceptable behavior of the classification that basically depends of the dense information found in the dataset, the classification path is modified to classify the image pixel by pixel. In such situation, each pixel value is compared with the mean value of each class in the dataset, and a similarity measure is computed between them, which indicate the class that the pixel belongs to. Accordingly, the resulted image was showed good classification.

The results assessment was carried out on the two classification paths by comparing the results with a reference classified image achieved by Iraqi Geological Surveying Corporation (IGSC). The comparison process is done pixel by pixel for whole the considered image and computing some evaluation measurements. It was found that the classification method was high quality performed and the results showed acceptable classification scores of about 70.64%, and it is possible to be approaches 81.833% when considering both classes: residential without vegetation and residential with vegetation as one class for SVD method. Also, the classification score was about 95.84% for the moment method. This indicates the ability of proposed methods to efficient classify multibands satellite image. The encouraging results gave the chance to suggest development problems for the present work to be better in the future when using another classification features for strengthing the classification results.

List of Contents

Chapter Two
Theoretical Concepts

Chapter Three
Proposed Satellite Image Classification Method

Chapter Four
Results and Analysis

Chapter Five
Conclusions and Future Work

List of Figures

List of Tables

List of Abbreviations

ANN	Artificial Neural Network.
B_{Max}	Maximum block size of image.
B_P	Three dimensional arrays represent the image blocks.
BDT	Binary Decision Tree.
D	Distance between two points.
ETM+	Enhance Thematic Mapper Plus.
ERDAS	Earth Resources Technology Satellite.
EMR	Electromagnetic Radiation.
EMS	Electromagnetic Spectrum.
ERTS	Earth Resources Technology Satellite.
IFOV	Instantaneous Field of View of the sensor.
IGSC	Iraq Geological Surveying Corporation
IR	Infrared Radiation.
LiDAR	Light Detection And Ranging.
MSS	Multispectral Scanner.
N_B	Number of blocks of image.
$\mathbf{N_C}$	Number of Cluster.
N_{Band}	Number of image bands.
OA	Overall Accuracy
OLI	Operational Land Imager.
PA	Producer Accuracy.
PCA	Principal Components Analysis.
QT	Quadtree partitioning method.
RADAR	Radio Detection And Ranging.
RBV	Return Beam Vidicon.
RGB	Red -Green- Blue.
ROI	Region of Interest.
RS	Remote Sensing
SIC	Satellite Image Classification.
SVD	Singular Value Decomposition
SVM	Support Vector Machine.
TIRS	Thermal Infrared Sensor.
TM	Thematic Mapper.
UA	User Accuracy.
UV	Ultraviolent.

CHAPTER ONE

GENERAL INTRODUCTION

CHAPTER ONE
GENERAL INTRODUCTION

1.1 Introduction

Remote sensing (RS) is the science of using electromagnetic radiations (EMR) to identify earth surface features and estimation of their geo- physical nature during analysis and interpretation of it's spectral, spatial, and temporal signature without doing physical contact with the object [Chi12]. RS uses satellite imagery technology to sense the landcover of Earth. At the early of stage 21st century, satellite imagery became widely available. Currently, various type of orbiting satellites are found to collect crucial data for improving knowledge about Earth's atmosphere, oceans, ice, and land. Orbital platforms used different regions of Electromagnetic Spectrum (EMS) to provide interest data, which contributed with larger scale aerial or ground-based sensing and analysis to prepare satellite images that picture enough information needed to monitor trends of natural phenomena [Bui93]. Satellite images are rich material that plays a vital role in providing geographical information [Sat11]. There are specialized RS applications are employed for interpreting and analyzing the satellite images in order to understand the behavior of considered phenomena [Add10].

Satellite Image Classification (SIC) is the most significant technique used in RS for the computerized study and pattern recognition of satellite information, which is based on diversity structures of the image that involving rigorous validation of the training samples depending on the used classification algorithm [Bab14]. The powerful of such algorithms is depends on the way of extracting the information from huge number of data found in images. Then, according to these information, the pixels are grouping into meaningful classes that enable to interpret and studying various types of regions that included in the image [Sun15].

1.2 Remote Sensing

Remote sensing is relevant process that permits to extract information about the surface of land without actual contact with the area being observed [Sam11]. The remotely sensed images are the aerial and satellite images that allow exact mapping of landcover and make landscape traits comprehensible on regional, continental, and even global scales [Ank14]. Figure (1.1) shows the principle of remote sensing, the solar radiation incident on objects found at the landcover, which are reflect these radiation toward the satellite, the satellite technology receive these radiation and record the image of the considered area [Har15].

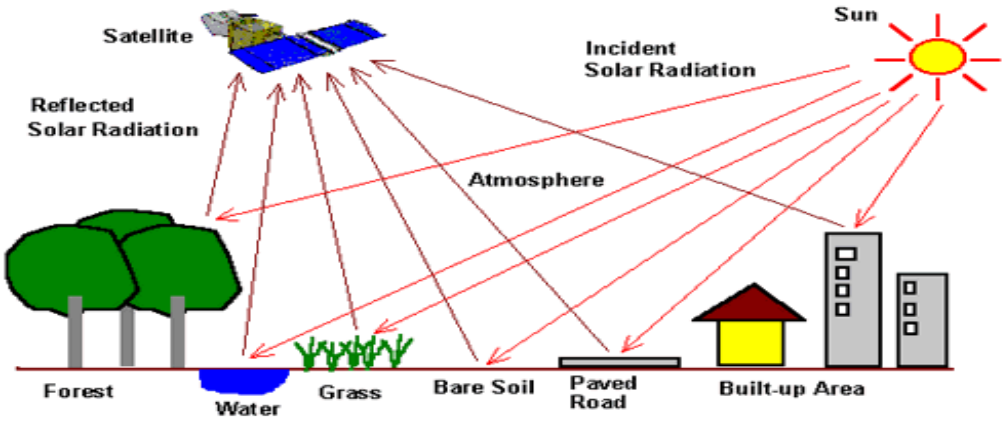

Fig (1.1) Principle of remote sensing [Hari15].

Remote sensing operates in several region of the electromagnetic spectrum. The ultraviolent (UV) portion of the spectrum has the shortest wavelength that is practical use of remote sensing. It is used to dig out a general picture for the object embedded underground. Passing through the visible spectrum, the infrared radiation (IR) is also used to record thermal images that are useful in climate consideration. Actually, satellite images are taken through the visible bands are usually employed in the appearance of digital images containing valuable information used to assist developers to understand the information of the

landcover. The aspires of satellite images categorization is to split image into discrete classes. The consequential classified image is a thematic map of the landscape image [Hari15]. The satellite imagery is categorized into active and passive remote sensing when information is merely recorded [May05], more details about them are given by the following subsections:

1.2.1 Active Remote Sensing

Active remote sensing emits radiation to scan objects and areas whereupon a sensor then detect and measures the radiation that is reflected or backscattered from the target as shown in Figure (1.2) [Mat08]. (Radio Detection And Ranging) RADAR and (Light Detection And Ranging) LiDAR are examples of active remote sensing where the time delay between emission and return signal is measured, which help to establish the location, speed and direction of the target object on the ground [Mat08].

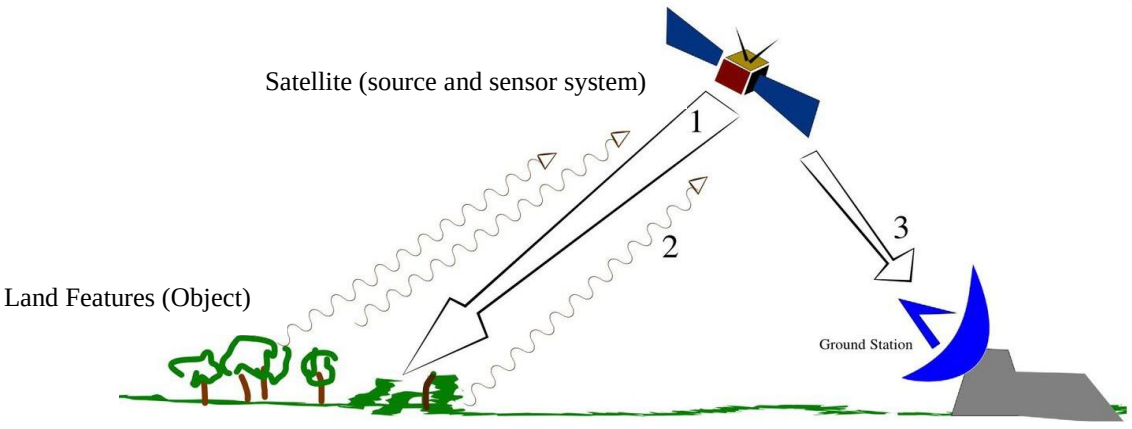

Fig (1.2) Active sensor system of remote sensing [Mat08].

1.2.2 Passive Remote Sensing

Passive sensors gather natural radiation that is emitted or reflected by the object or surrounding areas. The most common source of radiation measured by passive sensors is reflected sunlight as shown in Figure (1.3) [Mat08]. The common examples of passive remote sensing are satellite imagery, film photography, and radiometers [Lev99].

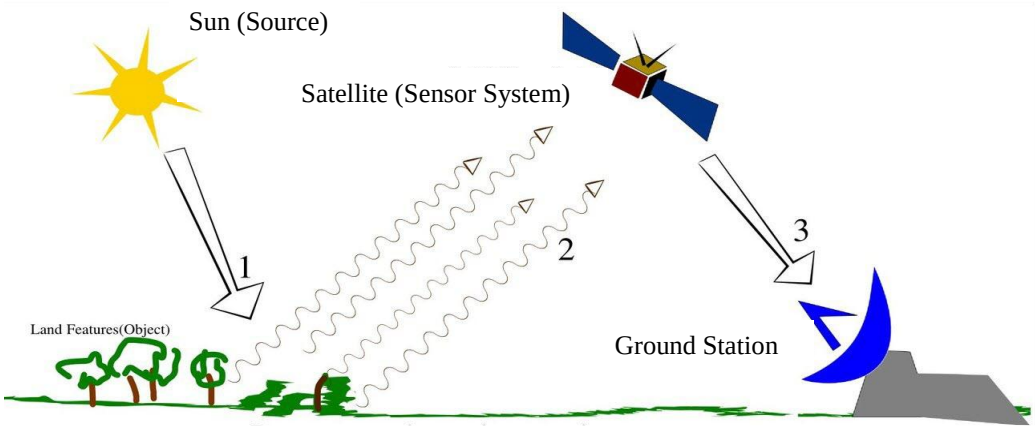

Fig (1.3) Passive sensor system of remote sensing [Mat08].

1.3 Satellite Imagery

Satellites are greatly used in the imagery purposes of remote sensing; they have several unique characteristics enable to sense the Earth's surface remotely. The satellite images are produced by sensing the electromagnetic energy at different wavelengths that reflected by objects. Visible satellite images are made via satellite signals received by visible channels that senses reflected solar radiation, such that, it is available only during daylight [Ren99]. The major benefit of using the visible imagery is due to its ability to give higher resolution images than other imagery bands. Thus, smaller features can be distinguished at visible imagery. The problem faces visible imagery is that clouds are white, while land and water surfaces are shaded, which impedes the process of satellite imagery. This problem is overcome by using radar sensors that uses microwaves to create satellite

image, such sensor is enabled to see through clouds and in night [Lil93]. On the other hand, optical sensors uses multispectral, hyper-spectral and multi-polarization technique that operated at different bands, which employed to improve the detection of objects under the sea or ground. Table (1.1) presents characteristics of the most popular optical satellites [ERD13].

Table (1.1) The most popular optical satellites [ERD13].

Satellite	**Mission life**	**Range resolution (*m*)**		
		Panchromatic	**Multispectral**	**Hyperspectaral**
IRS	1988 / 03	0.80	73.00	--
Landsat 7	1999 / 07	15.00	30.00	60.00
IKONOS	1999 / 09	1.00	4,00	--
RapidEye	1999 / 12	--	5.00	--
ASTER	1999 / 12	--	15.00	30.00– 90.00
MODIS	1999 / 12	--	250.00	500-1000
EROS	2000 / 12	0.50 – 0.90	--	--
QuickBird	2001 / 10	0.61	2.40	--
SPOT 5	2002 / 02	2.50 – 5.00	10.00	--
OrbView-3	2003 / 09	1.00	4.00	--
ALOS	2006 / 06	--	10.00	--
WorldView-1	2007 / 09	0.40	--	--
GeoEye-1	2008 / 09	0.41	1.65	--
WorldView-2	2009 / 06	0.41	1.80	--
Pleiades	2011 / 07	0.51	1.00	--

Many satellite platforms that used for imagery purposes are designed to follow a determined orbit in direction from north to the south of the earth, which corresponding to the Earth's rotation from the west to east. This setting of satellites allows them to cover most of the earth's surface over a certain period of time, where the coverage area is called swath [Lev99].

The Landsat (Land Satellite) provides the longest continuous record of satellite based observations. It is a primary source of medium spatial resolution Earth observations and monitoring global change .Observation requires revealing

both natural and human-induced landscape changes, Landsat provides the only inventory of the global land surface over time on a seasonal basis [Gya09].

1.4 Landsat Satellites

Landsat was designed in the 1960s and launched in 1972, The Landsat system is important in its own right as a remote sensing system that has contributed greatly to Earth resources studies. Landsat was proposed by scientists and implemented by U.S. government to satisfy applications of remote sensing to survey of the Earth's land areas. Then, Landsat became a project to lunch series of satellites as a part of National Aeronautics and Space Administration (NASA) Mission to Planet Earth that managed by the Goddard Space Flight Center in Greenbelt, which is a one of NASA's high priority programs to help further the understanding of the Earth system. The history of Landsat series is shown in Figure (1.4) [Jim96], whereas Table (1.2) mention mission dates of Landsat satellites.

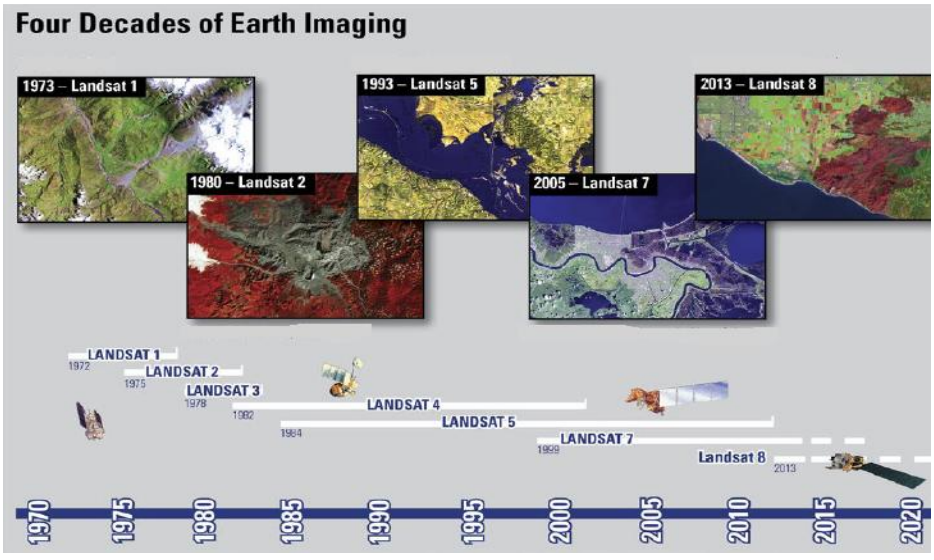

Fig (1.4) History of Landsat [Esh07].

Table (1.2) Landsat mission dates [Esh07].

Satellite	Launch	Decommissioned	Sensors
Landsat-1	July 23, 1972	January 6, 1978	MSS, RBV
Landsat-2	January 22, 1975	July 27, 1983	MSS, RBV
Landsat-3	March 5, 1978	September 7, 1983	MSS, RBV
Landsat-4	July 16, 1982	June 15, 2001	TM,MSS
Landsat-5	March 1, 1984	2013	TM,MSS
Landsat-6	October 5, 1993	Did not achieve orbit	ETM
Landsat-7	April 15, 1999	Operational	ETM+
Landsat-8	February 11, 2013	Operational	OLI/TIRS

The first Landsat sensor (Landsat-1) was known as the Earth Resources Technology Satellite (ERTS), it recorded energy in the visible and near infrared spectral. ERTS was practical for observation of Earth resources from satellite altitudes; it gives sufficient proportion of scenes that free of cloud cover [Noo15]. The Landsat system consists of spacecraft borne sensors that observe the Earth and then transmit information by microwave signals to ground stations that receive and process data for dissemination to a community of data users. Early Landsat vehicles carried two sensor systems: The Return Beam Vidicon (RBV) and the Multispectral Scanner Subsystem (MSS). The RBV was a camera like instrument designed to provide relative to the MSS, high spatial resolution and geometric accuracy but lower spectral and radiometric detail [Esh07].

1.5 Satellite Image Resolution

Satellite image resolution is the ability of sensor to monitor the smallest object clearly with distinct boundaries [ERD13]. Resolution often refers to a pixel count in digital imaging. It is described by the number of pixel columns (i.e., width of image) and the number of pixel rows (i.e., height of image). Pixel resolution indicates the squared area on the ground that covered by each pixel in the image, which is measured by one side of this square area. Table (1.3) [ERD13] list various pixel resolution for different satellites.

Table (1.3) Most interest satellite features [ERD13].

Feature	QuickBird	Landsat-7	GeoEye-1	IKONOS	World Veiw-2	Pleiades
GSD	0.6 *m*	15*m*	0.41 *m*	1*m*	0.5 *m*	0.5 *m*
Swath width	16.5*m*	185*km*	15*km*	13*km*	16.4*km*	20k *m*
Multispectral	Yes	Yes	yes	yes	yes	Yes
Revisit time (day)	3-4	16	2-3	1-3	2-3	2-3

In addition, there are four types of satellite image resolution may be taken in account, they are: spatial, spectral, radiometric, and temporal resolutions [Jay09]. More details for each type is given in the following subsections:

1.5.1 Spatial Resolution

Spatial resolution indicates the size of the smallest possible feature that can be pictured. In a digital image, the resolution is limited via the pixel size, i.e. the smallest resolvable object cannot be smaller than the pixel size. The essential resolution of an imaging system depends on their Instantaneous Field of View (IFOV) of the sensor, which is a measure of the ground area viewed by a single detector element in a given instant in time. The pixel size is determined by the sampling distance [Dap13].

1.5.2 Spectral resolution

Spectral resolution can be defined as the number of spectral bands used to record spectrally split radiative energy received from the target. Many remote sensing systems record energy over several separate wavelength ranges at various spectral resolutions. Advanced multi-spectral sensors called hyperspecteral sensors, which detect hundreds of very narrow spectral bands throughout the visible, near-infrared, and mid-infrared portions of the electromagnetic spectrum [Jay09].

1.5.3 Radiometric Resolution

Radiometric characteristics refer to the smallest change in intensity level that can be detected by the sensing system. A fine radiometric resolution is critical in studying targets that have only a subtle variation in their reflectance, such as detection of different kinds of minerals in the soil and varying levels of vegetation stress caused by drought and diseases. Also, remotely sensed data of a fine radiometric resolution are especially critical in quantitative applications in which a ground parameter (e.g., sea surface temperature and concentration level of suspended solids in a water body) is retrieved from pixel values directly. Data of a higher quantization level enable the retrieval to be achieved more accurately while a coarse radiometric resolution causes the pixels to look similar to each other [Jay 09].

1.5.4 Temporal resolution

Temporal resolution indicates the period at which the same ground area is sensed by the same sensing system. The actual temporal resolution is typically measured by days, it depends on three factors: satellite capabilities, swath overlap, and latitude. Since remote sensing satellites are revolving around the Earth 24 hours a day and 365 days a year, the temporal resolution is directly related to the satellite orbital period. A short period means more revolutions per day and is equivalent to a high temporal resolution [Jay09].

1.6 Satellite Image Classification

There are several methods and techniques for satellite image classification. Satellite image classification methods can be broadly classified into three categories: automated, manual, and hybrid as shown in Figure (1.5) [Sun15]: The following subsections illustrate each category of classification:

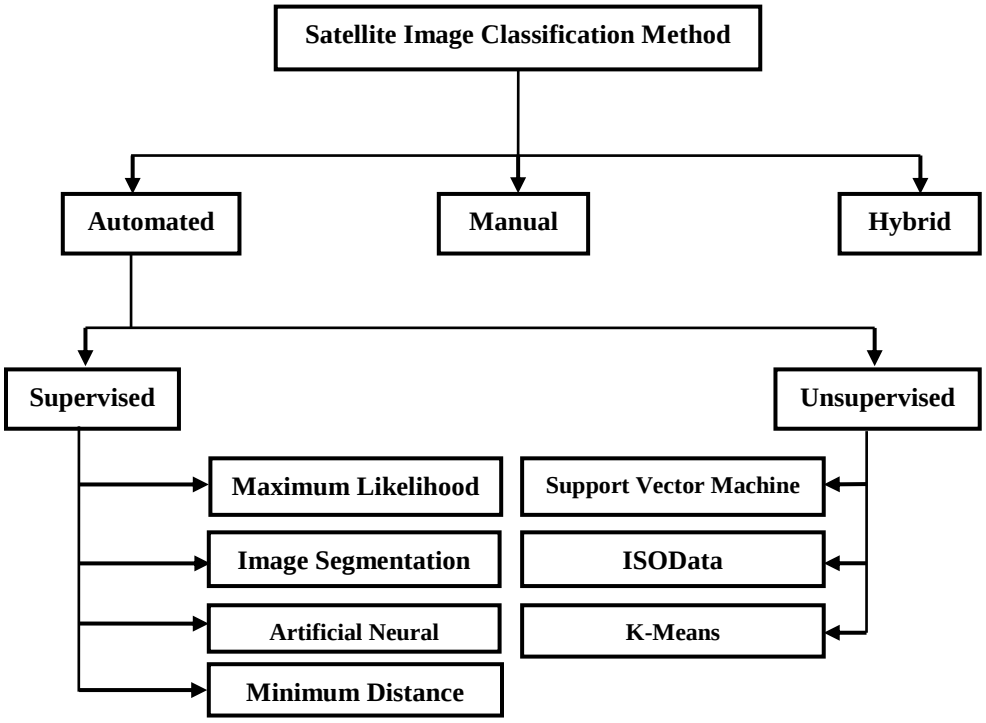

Fig (1.5) Satellite image classifications methods hierarchy [Sun15].

1.6.1 Automated Methods

Automated satellite image classification methods use algorithms that applied on the satellite image to systematically group pixels into meaningful categories. Majority of classification methods fall under this category. Automated satellite image classification methods further classified into two categories supervised and unsupervised classification methods [Sat11]; Figure (1.6) shows sequenced stages of both supervised and unsupervised that given in the following subsection.

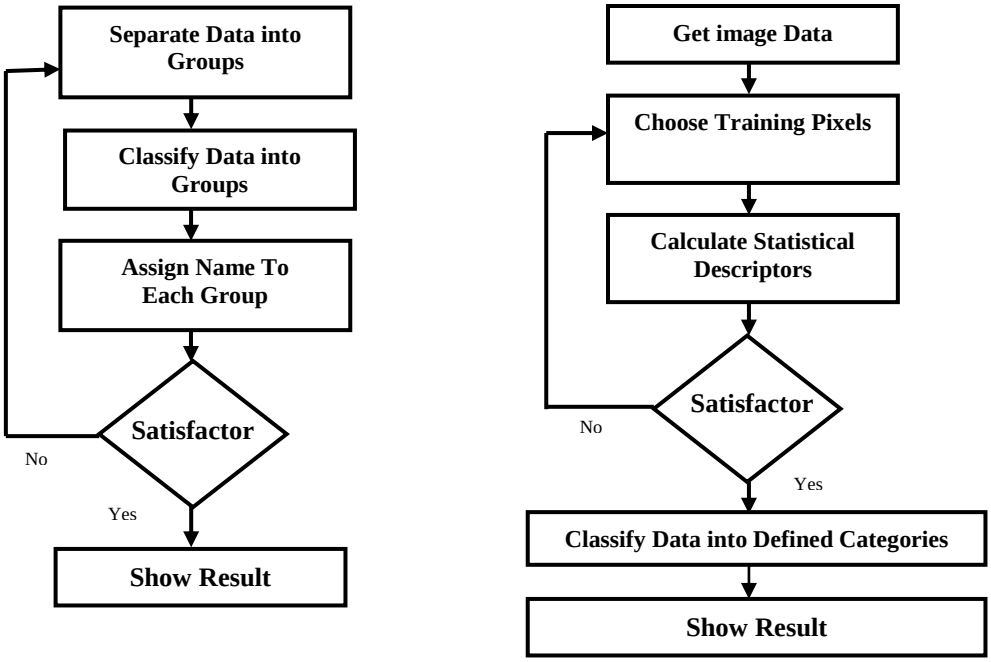

(a) Unsupervised Classification (b) Supervised Classification

Fig (1.6) Unsupervised and supervised classification principle [Sat11].

A. Unsupervised Classification

Unsupervised classification is a process of clustering satellite image pixels into unlabeled classes/clusters. The image classification concepts aids in unsupervised classification to provide an access into image features for clustering, which can be analyzed in term of classification quality. The result of an unsupervised classification is an image of statistical features clusters [Jia09]. There is several different unsupervised classification algorithms are commonly used in remote sensing. Most common ones of them are: isodata, support vector machine (SVM), and K-Means classification method that may be used to establish the dataset of the images that classified for first time [Sat11].

B. Supervised Classification

Supervised classification is a process of sorting pixels into a number of individual classes based on the comparison with training sets [Shi13]. Such methods require training set to be implemented, the data set predefined region of image belong to different classes in the image. The enrollment of the data set is an important primary stage in the supervised satellite image classification methods. The quality of a supervised classification depends on the quality of the training set. The supervised classification usually has the following sequence of operations: defining of the training sites, dataset (or, signatures) extraction, and image classification [Chr14]. Major supervised classification methods use the statistical techniques like Artificial Neural Network (ANN), Binary Decision Tree (BDT) and Image Segmentation [Sat11].

1.6.2 Manual Methods

Manual satellite image classification methods are robust, effective and efficient methods. This type of methods consumes more running time. In manual methods the efficiency and accuracy of the classification depend on knowledge and familiarity of the analyst towards the field of study [Sat11].

1.6.3 Hybrid Methods

Hybrid satellite image classification methods combines the advantages of automated and manual methods. Hybrid approach uses automated satellite image classification methods to get initial classification, further manual methods are used to refine classification and correct errors [Sun15].

1.7 Literature Survey

Several studies have been published in the field of interest; they mostly cover the use of satellite image classification methods. The following selected researches are the most interesting ones:

Rhonda, et al (2009) introduced a feature reduction method based on the singular value decomposition (SVD). This SVD-based feature reduction method reduces the storage and processing requirements of the SVD by utilizing a training dataset. This feature reduction technique was applied to training data from two multitemporal datasets of Landsat TM/ETM+ imagery acquired over a forested area in Virginia, USA and Rondônia, Brazil. Subsequent parallel iterative guided spectral class rejection (pIGSCR) forest/non-forest classifications were performed to determine the quality of the feature reduction. The classifications of the Virginia data were five times faster using SVD-based feature reduction without affecting the classification accuracy. Feature reduction using the SVD was also compared to feature reduction using principal components analysis (PCA). The highest average accuracies for the Virginia dataset (88.34%) and for the Rondônia dataset (93.31%) were achieved using the SVD. The results presented here indicate that SVD-based feature reduction can produce statistically significantly better classifications than PCA [Rho09].

Sathya P. **and Malathi** L. **(2011)** established a segmentation and classification of remote sensing images. This classified image is given to KMeans algorithm and Back Propagation algorithm of ANN to calculate the density count. The density count is stored in database for future reference and for other applications; also it has the capability to show the comparison of the results of both the algorithms. The experimental result found that K-means algorithm gives very high accuracy, but it is useful for single database at a time. The neural network provides good accuracy, and it found useful for multiple databases [Sat11].

Kumar et.al. (2012) proposed an improved contrast enhancement technique of multiband satellite image based on the singular value decomposition (SVD) and discrete cosine transform (DCT). Normalized difference vegetation index (NDVI) technique was used to extract features of low-contrast satellite images. The visual and quantitative results proved the increased efficiency and flexibility of the proposed method. The simulation results show that the enhancement-based NDVI using DCT-SVD technique is highly useful to detect the surface features of the visible area which are extremely beneficial for municipal planning and management [Ku12].

Aras (2014) Classified Landsat satellite images of the area of Laylan district in Kirkuk province, for the years 1990, 2000 and 2013 by using (ENVI 4.7, Matlab), several different methods of classification have been used to classify area of these images; like unsupervised method (ISODATA and K-Means), supervised methods (Mahalanibos distance classifier and Maximum likelihood Classifier) and scatter plot method to get the most accurate results and then to compare the results of each method. The result showed a growth in urban land between 1990 and 2013 while the vegetation witnessed a reduction in this period. The important observation is that the water bodies was not exist in selected area at the considered period but it appeared in 2013 image where the positive change happened in the top-left part of the selected area after the build of Shirin dam and collecting water there [Ara14].

Habib et al. (2014) used a Zernike moments-based descriptor as a measure of shape information for the detection of buildings from Very High Spatial Resolution (VHSR) satellite images. The proposed approach comprises three steps. First; the image is segmented into homogeneous objects based on the spectral and spatial information. Second; Zernike feature vector is computed for each segment. Finally, a Support Vector Machines (SVM) based classification using the feature vectors as inputs is performed. Experimental results and comparison with

Environment for Visualizing Images (ENVI) commercial package confirm the effectiveness of the proposed approach [Hab14].

Harikrishnan and Poongodi S. (2015) implemented a cellular with fuzzy rules for classifying the satellite image and analyzed the quality of classified image. cellular automata are implemented for simulation of satellite images and also cellular automata relates to categorization in satellite image is used simultaneously. Where the accuracy rate of cellular automata is very much increased when fuzzy rules are implemented to this systems, uncertain pixels which are still present in the classification process is eliminated and uncertain pixel is classified to each class its give paths to well classified image with high accuracy [Har15].

Akkacha et al (2015) proposed a combination of three classification methods which are K-means, LVQ (linear vector quantization) and SVM (support vector machine). The unsupervised k-means technique to get an initial view of the image site that will help to choose the best training area for SVM classification, which is the second kind. The last kind is the neuronal supervised LVQ technique. LANDSAT7 remote sensing images of the Ouargla oasis area were used. The results showed the vegetation separated from urban landscape. The neuronal LVQ method is also used in order to improve the opinion of base classifier when ensemble classification is done. It was noticeable that SVM gives the best results when using simple majority vote technique [Akk15].

Noor Z. **(2015)** established a satellite image classification based on semantic indexing techniques. After assurance the acceptable behavior of the classification, the results are evaluated and discussed for Landsat satellite image of Razaza Lake and the area surrounding district in Karbala province are classified for years 1990,1999 and 2014. It was found that water and hills in decrease, while vegetation, wet land and barren land in increase for years 1999 and 2014; comparable with 1990 and the results of proposed methods proved it's superiority, where the classification accuracies for the proposed method Singular Value

Decomposition are 92.5%, 89.5% and 90% for years 1990,1999,2014, respectivety, while it were 92%, 89% and 91% for unsupervised classification method based mean value in years 1990,1999,2014 receptively [Noo15].

Brindha S. (2015) proposed a satellite image enhancement using DWT-SVD, in which the image is segmented using the multiregional Resolution and the Markov Random Field (MRR-MRF) Model, this technique decomposes the input image into four frequency sub band by using DWT and also calculate the Singular Value Matrix of the Low-Low Sub band images and equalize the enhanced images through Inverse Discrete Wavelet Transform. After the enhancement process, image segmentation technique is applied to the image. MRR-MRF techniques to improve the segmentation accuracy, quality of the image, and reduce the noise of the satellite images. The experimental result showed better performance and high accuracy when compared with other methods [Bri15].

1.8 Aim of Thesis

The present work aims to classify satellite images using the k-means based singular value decomposition (SVD) method. The use of such method enables to study the concepts that concerned with enrollment phase. The study of training phase capabilities leads to improve the classification results. SVD is stand for supervised method depending on predefined dataset stored in the dictionary system that firstly established using the k-means. The optimal run of enrollment phase leads to create optimal dataset stored in the dictionary system and then used to determine intended classification results when the classification phase is used. Implies, the optimal choice of the training dataset indicates an optimal classification results.

1.9 Thesis Layout.

The thesis consists of five chapters; chapter one is a general introduction to the basic concepts related to the field of interest, also the most significant literatures are mentioned in details as well, and introduces the aim of the present thesis. Whereas the other four chapters are presented in the following:

Chapter Two, Entitled: Theoretical Concepts

This chapter introduces the specific concepts of satellite image classification methodology. The interesting classification techniques are explained with details; including methods of features extraction.

Chapter Three, Entitled: Proposed Satellite Image Classification Method

This chapter concerned with illustrating stages and steps of the proposed classification technique. The overall classification technique is described. Then, the mathematical explanation of each stage is given in details and presenting the related algorithms.

Chapter Four, Entitled: Result and Analysis

This chapter shows the test results of implementing the proposed technique. The results are presented and discussed to evaluate the performance of establish satellite image classification technique.

Chapter Five, Entitled: Conclusions and Future Work

This chapter contains a list of the derived conclusions as well as some suggestions for the future work related to the proposed technique.

CHAPTER TWO

THEORETICAL CONCEPTS

CHPTER TWO

THEORETICAL CONCEPTS

2.1 Introduction

Many applications uses satellite imagery are serving studies in different fields of science, such as: geosciences, astronomy and geographical information systems [Bri15]. These applications use image classification as an important tool to identify and detect most relevant information in satellite images [Ham11]. Satellite image classification is an extreme part of remote sensing that depends originally on the image resolution, which is the most important quality factor in images. Also, classification depends on extract and interpretation of valuable information from massive satellite images. Actually, satellite image classification is used for spatial data mining, information extraction, thematic map creation, visual interpretation, surveying field, effective decision making, disaster management, and others [Sun15].

This chapter introduces the fundamentals of satellite imagery classification. The mathematical descriptions of interest image processing are given to be useful for understanding the scientific reasons of choosing such technique. K-means and singular value decomposition (SVD) methods are the two methods of interest for image segmentation and classification in this study. The reason behind choosing these two techniques is that the K-means is one of efficient unsupervised learning algorithms that solve the well known clustering problem. Whereas the SVD is a numerical technique used to diagonalize matrices in numerical analysis, which is stable and effective method; also, it has the ability to adapt to the variations in local statistics of an image. The following sections explain the theoretical basis of the image classification based on methods of interest.

2.2 Image Segmentation

Segmentation refers to the process of partitioning a digital image into sub regions of pixels in order to simplify the representation. Different regions are more meaningful and easier to analyze [Sat11]. Image segmentation employed to determine location of objects or its boundaries in images. More precisely, it is a process of assigning a label to every pixel in an image such that pixels with the same label share certain visual characteristics. It represents the interface between image preprocessing and image understanding (i.e., object recognition). Results of image segmentation are a set of image segments that collectively covering the entire image [Bab14]. Image segmentation techniques can be divided into the following basic concepts: uniform partitioning and non-uniform partitioning, both are may be pixel oriented, contour-oriented, region-oriented, or hybrid [Sun15]. The following subsections explain the satellite image segmentation techniques of interest:

2.2.1 Uniform Partitioning

Uniform image partitioning is a process of dividing the image into square blocks of uniform size. This process does not concerned with the spectral distribution of the image, it is just geometrical partition. In such method, the size of block depends on the amount of spatial resolution of the image. Low resolution image is divided into a number of blocks is less than that of higher resolution image, this is for credit enough information are containing in each block. Figure (2.1) shows the uniform partitioning of a satellite image [Sal10].

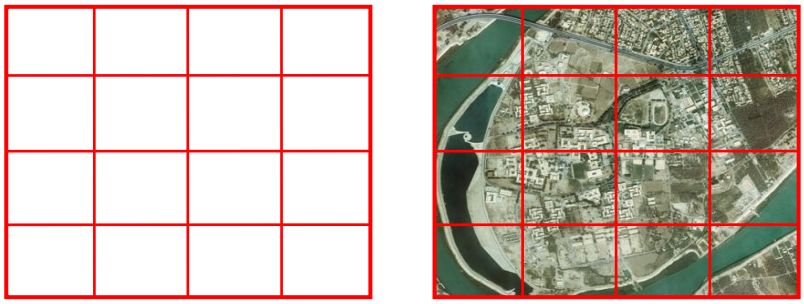

(a) Grid of Partitioning (b) Partitioning Image

Fig (2.1) Uniform partitioning of satellite image [Sal10].

2.2.2 Non-Uniform Partitioning

Non-uniform partitioning aims to divide the image into blocks of unequal size. The quadtree (QT) partitioning is the most confident method used for attaining this purpose. QT partitions the region of image into four equal root quarters, where each root is defined by three parameters: location, size and color. The partitioning process is further applying on each root to create four leaves; each leaf is regarded as new root and newly divided into four sub leaves. Figure (2.2) shows the process of image partitioning, which is continuing till a specific uniformity criterion is met or reaching a predefined minimum block size [Par12].

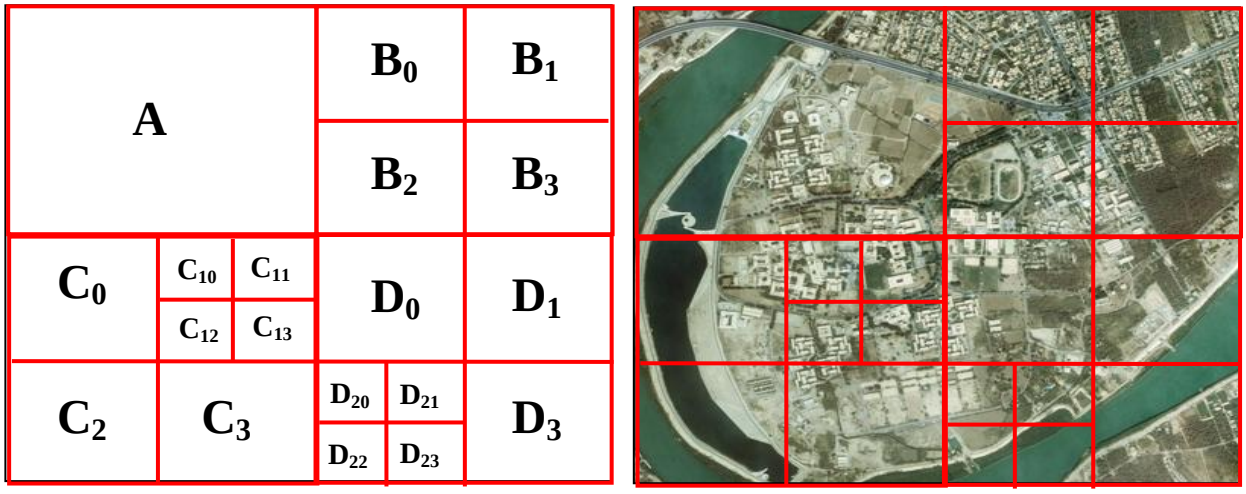

(a) Grid of Partitioning (b) Partitioning Image

Fig (2.2) Quadtree partitioning, the alphabetic letters refer to the root part and the number in subscript refer to the leaf parts [Par12].

The uniformity criterion is related to the variance of the current block. The variance is computed and then compared to a specific threshold in term of control parameters. The sequential steps of QT are given as follows [Abu02]:

1- Partition whole image into blocks whose size is equal to the maximum block size (roots) according to control parameters.
2- Check the uniformity criterion for each sub-block as follows:
   a- Compute the local mean of root block (m_s).
   b- Compute number of undesired pixels within each leaf (sub-block) (N_p), which may differ from the mean value (m_s) by distance more than (σ_e), those pixels satisfy the value (1) in the following condition:

$$Np = \sum_{i=1}^{M}\sum_{j=1}^{N}\begin{cases}1 & |f(i,j) - m_s| > \sigma_e \\ 0 & |f(i,j) - m_s| \le \sigma_e\end{cases} \quad \dots (2.1)$$

Where, *f (i,j)* is pixel value, *M* block height and *N* is block width.

   c- If the ratio of undesired pixels (Np/S), where S is the block size, is less than the acceptance ratio then the block do not partitioning, otherwise the block should be partitioning into four sub-blocks.

This procedure was repeated until the uniformity condition is satisfied or the sub-block reaches to the minimum size.

QT have nodes either are parent root with or without four children or leaves. Each leaf represents a block of pixels in the image. A single value is used by the leaf to represent the entire block; this value is the average (A_P) value of the pixels within the block. The average pixel value within a block is defined by the equation [Saliha and Slimane, 2010],

$$A_P = \frac{1}{S^2}\sum_{i=b}^{b+S-1}\sum_{j=a}^{a+S-1} f(i,j) \quad \dots (2.2)$$

Where (a, b) is the location of the lower corner of the leaf, and S is the width and height of the block represented by the leaf [Luk13]. The partitioning process utilizes the spectral variety condition to partition the image into blocks. Accordingly, the target image is partitioned into many blocks depending on the variety of the local gray in each block, which depend basically on the local mean (μ) and standard deviation (σ) of both the root and its four leaves those given in the following equations: [Ani11]

$$\mu = \frac{1}{W \times H} \sum_{i=0}^{W-1} \sum_{j=0}^{H-1} f(i,j) \quad \text{... (2.3)}$$

$$\sigma = \sqrt{\frac{1}{W \times H} \sum_{i=0}^{W-1} \sum_{j=0}^{H-1} (f(i,j) - \mu)^2} \quad \text{... (2.4)}$$

2.3 Image Classification

Classification is a data mining method is used to classify the image into predefined group. Classification is performed when the image needs to be assigned into a predefined classes based on a number of observed attributes related to that image [Ana14]. This refers to the task of extracting information from satellite image; the information is assigned into classes according to specific features that distributed in the image. The classified image is shown as a colored map like Figure (2.3). Classification process of an image is usually carried out after segmenting the image into spectral uniform regions [Jen05]. Several methods of image classification exist and a number of fields apart from remote sensing like image analysis and pattern recognition make use of classification. In other cases, the classification can serve only as an intermediate step in more intricate analyses, such as land-degradation studies, process studies, landscape modeling, coastal zone management, resource management and other environment monitoring applications. Classification of a satellite image can be achieved by unsupervised or supervised procedures [Par14].

(a) Original Satellite Image (b) Classified Satellite Image

Fig (2.3) Satellite image classification [Has07].

Satellite image classification needs mainly to perform the: segmentation first. The objective of image segmentation is equivalent to unsupervised classification, which going to partition the image into parts of strong correlation with areas of the real world contained in the image. Image segmentation is typically carried out as a preprocessing step for some landcover and landuse classification systems [Ank14]. Lot of classification algorithms presented in data mining and artificial intelligence have been extensively used, some of them are pixel oriented, while the others are block or region oriented methods. Generally, classification of remotely sensed imagery is a challenging subject because of the complexity of landscapes, the spatial and spectral resolution of the images being employed. A multispectral remotely sensed image comprises information collected over a large range of variation in frequencies and these frequencies vary over diverse [Ank14].

2.4 K-Means Clustering

K-means is one of the effective unsupervised learning methods that solve the clustering problem. This method keep track of classify a given data set through a certain number of clusters (assume *k* clusters) fixed a priori. The main idea is to define *k* centroids, one for each cluster. These centroids are separated at different locations; the better choice is to place them as much as possible far away from each other. Then, each point belonging to a given dataset is associated to the nearest centroid. When no point is pending, new *k* centroids of the clusters re-calculate, and new binding has to be done between the same data set points and the closest new centroid. A loop has been generated; the result of this loop is change locations of the *k* centroids step by step until no more changes are done. Implies, centroids do not move any more due to minimizing an objective function to be minima [Sat11].

The application of this algorithm on digital image requires being starts with some clusters of pixels in the feature space, each of them defined by its center. The first step is allocating each pixel to the nearest cluster, while the second step is computing new centers with new clusters. These two steps are repeated until convergence. Therefore, the k-means algorithm adopts the following three steps till reaching the final state [Sat11].

1. Determine the centroid coordinate.
2. Determine the distance of each object to the centroid.
3. Group the object based on minimum distance.

2.5 Singular Value Decomposition

Singular value decomposition (SVD) is useful factorizations method in linear algebra [Nei04]. SVD can be used in computer vision as a decomposition matrix as a tool for exploratory data analysis, data processing and compression [Nag12]. It is a single numerical feature provides a quantitative assignment for query image to the closest class [Asw14]. The *SVD* is an attractive algebraic transform for image

processing applications. It is a stable and effective method to split the system into a set of linearly independent components, each of them bearing own energy contribution [Rho09]. It can be considered as a generalization of the eigen decomposition of square matrices, to analyze rectangular matrices [Pra10].

SVD technique is based on a theorem of linear algebra that mentions; a rectangular $m \times n$ matrix A having m rows and n columns in which $m \geqslant n$, is can be factorize into the product of three matrices, [Bha11] as given in Equation (2.5) [Bri15].

$$A = USV^{\mathbf{T}} \quad \ldots (2.5)$$

Where U is a $m \times n$ matrix of the orthonormal eigenvectors of AA^T called the left singular vectors of A satisfy equation (2.6), V^T is the transpose of a $n \times n$ matrix containing the orthonormal eigenvectors of $A^{\boldsymbol{T}}A$ called the right singular vectors of A satisfy equation (2.7), $I_{n\times n}$ and $I_{p\times p}$ are the identity matrices of size n and p, respectively, and S is a $n \times n$ diagonal matrix with nonnegative diagonal entries of the singular values which are the square roots of the eigenvalues of $A^{\boldsymbol{T}}A$ and called the singular values of A, which given in equation (2.8) [Ran14], as follows:

$$U^{\mathbf{T}}U = I_{n\times n} \quad \ldots (2.6)$$

$$V^{\mathbf{T}}V = I_{p\times p} \quad \ldots (2.7)$$

$$S = \begin{bmatrix} \sigma_1 & 0 & \cdot & 0 & 0 \\ 0 & \sigma_2 & \cdot & 0 & 0 \\ 0 & 0 & \cdot & 0 & 0 \\ \cdot & \cdot & \cdot & \cdot & \cdot \\ 0 & 0 & . & \sigma_{n-1} & 0 \\ 0 & 0 & . & 0 & \sigma_n \end{bmatrix} \quad \ldots (2.8)$$

Where $\sigma_1 \geq \sigma_2 \geq \cdots \geq \sigma_p$, $p = \min\{m, n\}$, and $U=[u_1 \quad \ldots \quad u_m]$, $V=[v_1 \quad \ldots \quad v_n]$.

In order to implement singular value decomposition it is necessary to find the eigenvalues and eigenvectors of the symmetric matrices $A^{\boldsymbol{T}}A$ and $A\,A^{\boldsymbol{T}}$. The eigenvectors of $A^{\boldsymbol{T}}A$ are the columns of matrix V. such that, the matrix $A^{\boldsymbol{T}}A$ can be written as:

$$A^T A = USV^T VSU^T = US^2U^T \quad \dots (2.9)$$

The eigenvectors of AA^T make up the columns of matrix *U*. The matrix AA^T can be written as [Amm13]:

$$AA^T = USV^T VSU^T = US^2U^T \quad \dots (2.10)$$

Finally, the singular values in *S* are the square roots of the matrix AA^T or $A^T A$ eigenvalues. The singular values are arranged in descending order on the primary diagonal of matrix *S*. These singular values are real numbers. More explicitly, if *A* is a matrix with real values, then the values in *U* and *V* are also real [Chr14].

To compute SVD one can use the Jacobi method for symmetric matrices known as the "one-sided Jacobi method for SVD" that determined d_1, d_2, and c = cos (θ), and s = sin (θ) such that [Nei04]:

$$\begin{bmatrix} d_1 & 0 \\ 0 & d_2 \end{bmatrix} = \begin{bmatrix} c & -s \\ s & c \end{bmatrix} \begin{bmatrix} \sum_{k=1}^{m} u_{k,i}^2 & \sum_{k=1}^{m} u_{k,i}u_{k,i} \\ \sum_{k=1}^{m} u_{k,i}u_{k,i} & \sum_{k=1}^{m} u_{k,i}^2 \end{bmatrix} \begin{bmatrix} c & s \\ -s & c \end{bmatrix} \quad \dots (2.11)$$

Where *c* and *d* used as indices rotation matrix that acts on columns *i* and *j* during right multiplication, and the singular value σ_i can be compute as follows [Nei04]:

$$\sigma_i = \sum_{k=1}^{m} u_{k,i}^2 \ , \ i = 0 \dots n \quad \dots (2.12)$$

The algorithm requires a tolerance ε to control termination. It is suggested that ε be set to a small multiple of the unit round off precision (ε_o). Appendix (A) shows a simple example for computing the *SVD*.

2.6 SVD Properties

The main advantage of *SVD* is its more resistant to scaling, translation and rotation attacks class [Asw14]. Also, there are many useful properties and attributes of *SVD* are given in the following [Mee14]:

1. Stability: The SVD have a strong stability since the variation of both original and disturbed SVD cannot exceed 2-norm of the difference between the original and modified matrices.
2. Invariance to geometric distortions: The SVD exhibits the geometric invariance can be expressed in the structure matrices of SVD representation.
3. Translational invariance: Both the matrix A and its translated counterpart has same singular values.
4. Flip invariance: Both the matrix A and its flipped counterparts have same singular values.
5. Transposition: Both matrix A and its transpose have same singular values.
6. The rank of matrix A is equal to the number of its nonzero singular values.

2.7 Moment Based Classification

In physics, the concept of moment is derived from Archimedes' discovery of the operating principle of the lever. In the lever one applies a force, in his day most often human muscle, to an arm, a beam of some sort. Archimedes noted that the amount of force applied to the object (i.e., moment) is defined as the following equation:

$$M = r^s \times F \quad \dots (2.13)$$

Where *F* is the applied force, and *r* is the distance from the applied force to object and s is the order of the moment [Bal88]. In mathematics, a moment is a specific quantitative measure, used in both mechanics and statistics, of the shape of a set of points. If the points represent mass, then the zeroth moment is the total mass, the first moment divided by the total mass is the center of mass, and the

second moment is the rotational inertia. If the points represent probability density, then the zeroth moment is the total probability (i.e. one), the first moment is the mean, the second central moment is the variance, the third moment is the skewness, and the fourth moment (with normalization and shift) is the kurtosis . The mathematical concept is closely related to the concept of moment in physics [Ily13].

Therefore, the moment is a physical measure refers to the rotation effect of any external force like mechanical, electric, or magnetic force applied on body around an axis. In principle, any physical quantity can be multiplied by distance to produce a moment. In image processing, the pixel value acts as a force and the distance is measured between the pixel and a specific center. The quantity of determined moment depends on the color value of the pixel and its distance from the origin [Ballanda, 1988]. One can also define first moment, second moment…, or n^{th} moment depending on the power of distance used to compute the moment [Ily13].

CHAPTER THREE

PROPOSED SATELLITE IMAGE CLSSIFICATION METHOD

CHAPTER THREE
PROPOSED SATELLITE IMAGE CLSSIFICATION METHOD

3.1 Introduction

Satellite image classification (SIC) is a process of describing the contents of landcover digital image according to pre-established meaningful legend. This requires first to visually analyze the image to suggest the proper method of classification. There are many different techniques used in analyzing images. Each technique may be useful for a small range of tasks, there still aren't any known methods of image analysis that are generic enough for wide ranges of tasks, compared to the abilities of a human's image analyzing capabilities. Such that, the analysis task is usually done visually, then the classification is automatically carried out. Image classifier refers to computer program used to implement a specific procedure that will best accomplish a specific task. There are many classification techniques in literature survey used for different purpose given by various researchers; mostly they have been classified as either supervised or unsupervised methods. Supervised techniques are often required input from an analyst known as training set, which required sort of prior knowledge in selecting correct region of interest (ROI), whereas the unsupervised methods need to identify the correct number of regions existed in the processed image and no training set are required.

This chapter is concerned with explanation the use of K-means for enrollment the dataset and the use of SVD as an effective tool to establish SIC. The generic structure of the proposed SIC is presented in details; each stage in the proposed system is discussed and explained by editing its algorithm that based on the basis mentioned in previous chapters.

3.2 Proposed SIC Method

The concept of multi-stage query processing and preparing the dataset has been used to model the proposed method. It is claimed that these stages can beneficially be combined and through the combination, a significant fast and efficient satellite image classification can be achieved.

The generic structure of the proposed satellite image classification using K-means based SVD method described in Figure (3.1). It is shown that the proposed method is designed to be consisted of two phases: enrollment and classification. The enrollment phase goes to collect the training dataset (referred as *A*), which an offline phase that responsible on collecting sample image classes to be stored in dataset matrix to be a comparable models. Whereas the classification phase is an online phase responsible on verifying the contents of the test image in comparison with the trained models found in the dataset, this phase depends on the dataset created by the enrollment phase. Both phases are composed of three preprocessing stages include: image composition, image transform and preparing. Then, the enrollment includes sequenced stages of image partitioning, feature extraction and then clustering to establish the dataset. On the other hand, the classification phase includes stages of either block oriented classification or pixel oriented classification methods. Each of them consist of sequenced stages aims to extract the classification features from the employed image unit (pixel or block). In addition, there are an intermediate stages included in the classification are used to achieve the intended purpose are shown in Figure (3.1) and described in the following sections.

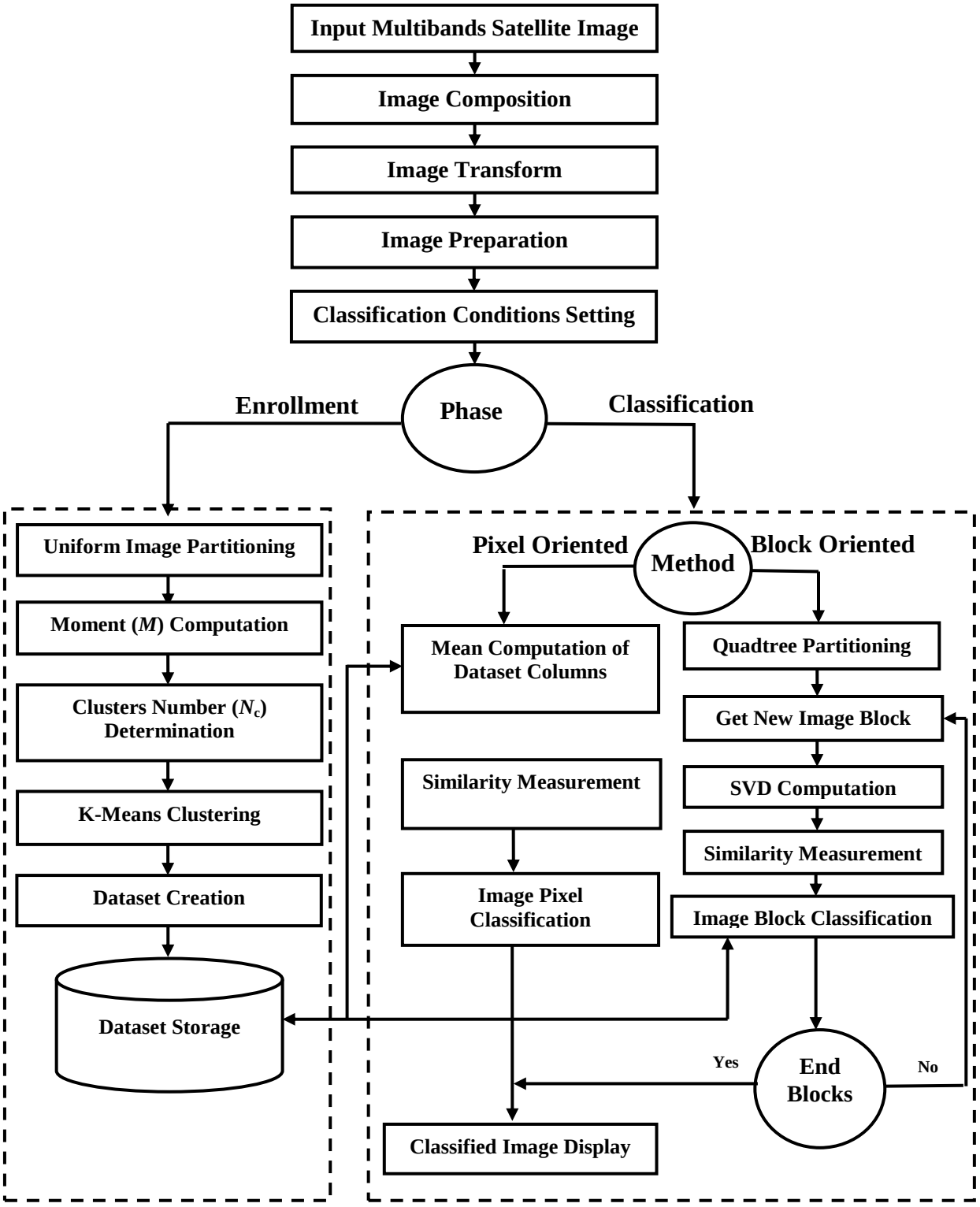

Fig (3.1) Block diagram of the proposed SIC method.

3.3 Image Composition

Satellite image is usually taken in multibands; this stage is aiming to compose the most informatic three bands in one color image given in RGB color space. The dispersion coefficient (*D*) of the whole image *f* (*i*,*j*) that given in equation (3.1) is used as a measure for quantifying whether a set of observed details are clustered or dispersed compared to a standard case. This parameter indicates the amount of the information found in each band. The three bands of greatest value of *D* are chosen to be combined with each other to make the composed image $F_{R,G,B}(i, j)$ employed in the following.

$$D_k = \frac{\sigma^2}{\mu} \quad \text{..... (3.1), [John, 2016]}$$

Where, μ and σ^2 are the mean and variance of k^{th} band of satellite image of W×H resolution as given in equations (2.3 and 2.4). Such that, the green band F_G, red band F_R, and blue band F_B are given as follows:

$$F_G(i,j) = \text{Max}_{\text{First}}(\text{D}_\text{k}) \quad \text{..... (3.2)}$$

$$F_R(i,j) = \text{Max}_{\text{Second}}(\text{D}_\text{k}) \quad \text{..... (3.3)}$$

$$F_B(i,j) = \text{Max}_{\text{Third}}(\text{D}_\text{k}) \quad \text{..... (3.4)}$$

Figure (3.2) illustrates the algorithm of the image composition.

Fig (3.2) Image composition.

Algorithm: Image composition

Input:

F (i, j, k) \\ Three dimension array represents the six band image.

N_{Band} \\ Number of image bands.

Output:

$F_G(i,j)$ \\ Green component of composed image.

$F_R(i,j)$ \\ Red component of composed image.

$F_B(i,j)$ \\ Blue component of composed image.

Procedure:

Loop for k=*1* ***to*** N_{Band}

Set s ← 0

Loop for i=0 ***to*** W-1

Loop for j=0 ***to*** H-1

Set s ← s + F (i, j, k)

End loop // j

End loop // i

Set M_u ← s / (W× H)

Set s ← 0

Loop for i=0 ***to*** W-1

Loop for j=0 ***to*** H-1

Set s ← s + (F (i, j, k) -M_u)^2

End loop //j

End loop //i

Set S_g ← s / (W× H)

Set D (k) ← S_g / M_u

End loop //k

//K_1 is the index of first Max Value of D (k).

//K_2 is the index of second Max Value of D (k).

//K_3 is the index of third Max Value of D (k).

Loop for i=0 ***to*** W-1

Loop for j=0 ***to*** H-1

Set F_G (i,j) ← F (i, j, k_1)

Set F_R (i,j) ← F (i, j, k_2)

Set F_B (i,j) ← F (i, j, k_3)

End loop //j

End loop //i

3.4 Image Transform

This stage is an important one for concentrating the information carried in three bands to be dense in one grey band. Thus, the three estimated bands F_R, F_G, and F_B are converted into single bands according to YIQ color transformation system. The *Y* represents the intensity band, whereas both *I* and *Q* represent the chrominance bands. Just the *Y* band is useful in the present work, which can be noted as F_T and estimated according to the following relation:

$$F_T(i,j)=0.299\ F_R(i,j)+0.587\ F_G(i,j)+0.114F_B(i,j) \quad \ldots\ldots \text{ (3.5), [Gonzalez, 2001]}$$

Figure (3.3) illustrates the algorithm of image transform.

Fig (3.3) Image transform.

Algorithm: Image transform

Input:

$F_G(i,j)$ \\ Green component of composed image.

$F_R(i,j)$ \\ Red component of composed image.

$F_B(i,j)$ \\ Blue component of composed image.

Output:

$F_T(i,j)$ \\ Two dimensional array represents the transform image.

Procedure:

Loop for i=0 ***to*** W-1

Loop for j=0 ***to*** H-1

Set $F_T(i,j) \leftarrow 0.2989*F_R(i,j) +0.5870*F_G(i,j) +0.114*F_B(i,j)$

End loop //j

End loop //i

3.5 Satellite Image Preparation

This stage is regarded to increase the contrast of the given material image. It is necessary when the used image is not employed all the color range that specified for the imaging process in the satellite. This case is happen when the illumination condition are not compatible to the optimal situation. Contrast stretching is used to enhance the appearance of image details, which can be achieved by adopting the linear fitting applied on the input image F_T for achieving the output image F_P as given in the following equation:

$$F_P = aF_T + b \quad \text{... ..... (3.6)}$$

Where, a and b are the linear fitting coefficients given in the following equations, in which Min_1 and Max_1 are the minimum and maximum values of pixels found in transformed image, whereas Min_2 and Max_2 are the intended values of the minimum and maximum of output image pixels. Figure (3.4) illustrates the algorithm of image preparation.

$$a = \frac{\begin{vmatrix} Max_2 & 1 \\ Min_2 & 1 \end{vmatrix}}{\begin{vmatrix} Max_1 & 1 \\ Min_1 & 1 \end{vmatrix}} \quad \text{... ..... (3.7)}$$

$$b = \frac{\begin{vmatrix} Max_2 & Max_1 \\ Min_2 & Min_1 \end{vmatrix}}{\begin{vmatrix} Max_1 & 1 \\ Min_1 & 1 \end{vmatrix}} \quad \text{... ..... (3.8)}$$

Fig (3.4) Image preparation.

Algorithm: Image preparation

Input:

F_T (i, j) \\ Two dimensional array represents the transform image.

Min_2 \\ Minimum value wanted in the prepared image.

Max_2 \\ Maximum value wanted in the prepared image.

Output:

F_P (i, j) \\ Two dimensional array represents the prepared image.

Procedure:

Set $Min_1 \leftarrow$ Min (F_T (i, j))

Set $Max_1 \leftarrow$ Max (F_T (i, j))

Set a $\leftarrow$ (Max_2 - Min_2) / (Max_1 - Min_1)

Set b $\leftarrow$ ($Max_2 * Min_1 - Max_1 * Min_2$) / ($Max_1$ - Min_1)

Loop for i=0 ***to*** W-1

Loop for j=0 ***to*** H-1

Set F_P (i, j) $\leftarrow a * F_T$ (i, j) + b

End loop //j

End loop //i

3.6 Classification Conditions Setting

In this stage, the intended conditions of classification status are determined. This conditions are used in both enrollment and classification phases. For the partitioning stage, the maximum block size (B_{Max}) and minimum block size (B_{Min}) are set at the situation that gave best classification results because there is no rule can be used to determine the optimal block size (try and error).

3.7 Enrollment Phase

The enrollment of dataset is an important step in the image classification. It is used for determining the image classes depending on sequenced stages. It is intended to partition the image and use the moment as the feature that represents each part. K-Means algorithm is used for grouping these features and to determine the best similar clusters (centroids). The image part belongs or closes to each centroid are stored in dataset array to be used in the classification phase. The following subsections explain more details about stages of enrollment phase:

3.7.1 Uniformly Image Partitioning

In this stage, the prepared image (F_P) is uniformly partitioned into equal blocks of size B_{Max}. The reason of using B_{Max} is to make the dataset containing greater number of information related to each class. This dataset can resized and scaled down to be half or quarter B_{Max} as needed in the classification. The average of the two successive elements gave new value in the half scaled down dataset, and another averaging leads to get quarter scaled down for the dataset. Figure (3.5) illustrates the algorithm of the uniform image partitioning.

Fig (3.5) Uniform Image partitioning.

Algorithm: Uniform Image partitioning

Input:

F_P (i, j) \\ Two dimensional array represents the prepared image.

B_{Max} \\ Side length of squared image block (F_P).

Output:

B_P \\ Three dimensional array represents the image blocks.

Procedure:

Set k← 0

Loop for i=0 ***to*** W-1 step B_{max}

```
Loop for j=0 to H-1   step Bmax
    Set k← k+1
    Set Si (k) ← i
    Set Sj (k) ← j
    Loop for x=0 to Bmax-1
      Loop for y=0 to Bmax-1
          BP (x, y, k) ← FP (i+x, j+y)
      End loop //y
    End loop //x
  End loop //j
End loop //i
```

3.7.2 Moment Computation

The Moment is a specific quantitative measure used to represent the information found in each image block. The shape of a set of pixels is a distribution of mass, which can be described by first-ordered moment given in equation (2.13), where the applied force (F_P) represented the pixel of block and r is the distance from the applied force to the center of block.

In such case, the pixel value (F_P) is regarded as the meant force, while the distance (D_s) is determined depends on the position of each pixel, if the pixel falls in the first quarter then the distance (D_{s1}) can be computed as shown in Figure (3.6-a) by using equation (3.9), and if the pixel falls in the second quarter then the distance (D_{s2}) can be computed as shown in Figure (3.2-b) by using equation (3.10), if the pixel falls in the third quarter then the distance (D_{s3}) can be computed as shown in Figure (3.2-c) by using equation (3.11), and if the pixel falls in the fourth quarter then the distance (D_{s4}) can be computed as shown in Figure (3.2-d) by using equation (3.12).

The moment of each block can be determined as shown below:

1. Compute the Euclidean distance D_s between each pixel of a specific block and the center of that block (the difference between the pixel and the center of block) as follows:

   a. If the pixel $F_P(i, j)$ falls in the First quarter then the D_s is computed by using the following relation:

   $$D_{s1} = \sqrt{(|i - i_o| - 0.5)^2 + (|j - j_o| - 0.5)^2} \quad \ldots\ldots (3.9)$$

   b. If the pixel $F_P(i, j)$ falls in the Second quarter then the D is computed by using the following relation:

   $$D_{s2} = \sqrt{(|i - i_o| - 0.5)^2 + (|j - j_o| + 0.5)^2} \quad \ldots\ldots (3.10)$$

   c. If the pixel $F_P(i, j)$ falls in the Third quarter then the D is computed by using the following relation:

   $$D_{s3} = \sqrt{(|i - i_o| + 0.5)^2 + (|j - j_o| - 0.5)^2} \quad \ldots\ldots (3.11)$$

   d. If the pixel $F_P(i, j)$ falls in the Fourth quarter then the D is computed by using the following relation:

   $$D_{s4} = \sqrt{(|i - i_o| + 0.5)^2 + (|j - j_o| + 0.5)^2} \quad \ldots\ldots (3.12)$$

   Where i_0, j_0 are represent the indices of the center block.

2. Compute the moment $M_p\ (i, j)$ of each pixel in a specific block of image by using the following relations:

   $$M_p\ (i, j) = F_P\ (i, j) * D_s \quad \ldots\ldots (3.13)$$

3. Compute the moment of a specific block (M) in image by using the following relation:

   $$M = \frac{1}{B_h * B_w} \sum_{i=0}^{B_h} \sum_{j=0}^{B_w} M_p(i, j) \quad \ldots\ldots (3.14)$$

   Where B_h *is* the height of block and B_w is the width of block.

Where M_p (i, j) represent the moment of pixel in a specific block of image, and $F_P(i,j)$ represent the pixel value of a specific block at position (i,j), i, and j are indices of the pixel in block of image, D_s represent the Euclidean distance. Figure (3.7) illustrates the algorithm of the moment computation.

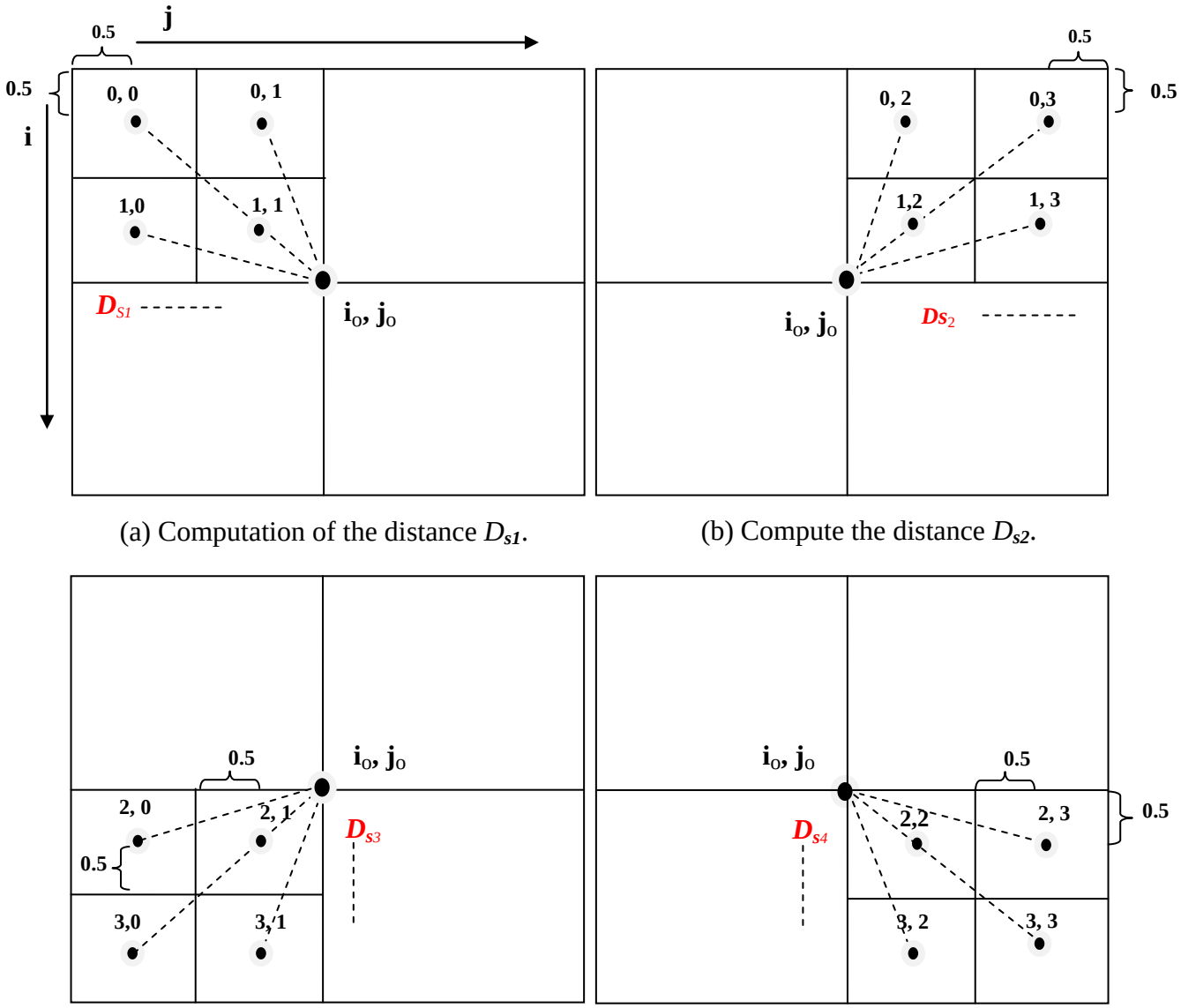

(a) Computation of the distance D_{s1}.

(b) Compute the distance D_{s2}.

(c) Compute the distance D_{s3}.

(d) Compute the distance D_{s4}.

Fig (3.6) Schematic description for computing the distance D_S for cases (a, b, c and d).

Where i, j are indices of pixel and i_o, j_o are indices of the center block.

Fig (3.7) Moment Computation.

Algorithm: Moment Computation

Input:

B_P \\ Three dimensional array represents the image blocks.

B_{Max} \\ Side length of squared image blocks (F_P).

S_i \\ 1D array refer to the horizontal portion of block in the image.

S_j \\ 1D array refer to the vertical portion of block in the image.

N_B \\ number of image blocks in the image ($N_B = (W \times H)/B_{max} \times B_{max}$).

Output:

M \\ 1D array represent the moment of the blocks.

Procedure:

Loop for k=1 ***to*** N_B

Set i← S_i (k) Set j← S_j (k)

Set i_o← i+ (B_{Max}/2)

Set j_o← j+ (B_{Max}/2)

Set D← 0.0

Set Sum ← 0

Set h ← 0.5

Loop for x=i ***to*** (i+B_{Max})

Loop for y=j ***to*** (i+B_{Max})

If (x< i_0) And (y < j_0) ***then***

D ← Sqr ((Abs (x - i_0) - h) ^{2} + (Abs (y - j_0) - h) ^{2})

Else If (x> i_0) And (y < j_0) ***then***

D ← Sqr ((Abs (x - i_0) - h) ^{2} + (Abs (y - j_0) +h) ^{2})

Else If (x< i_0) And (y > j_0) ***then***

D ← Sqr ((Abs (x – i_0) + h) ^{2} + (Abs (y – j_0) - h) ^{2})

Else If $(x>i_0)$ And $(y>j_0)$ ***then***

$D \leftarrow Sqr((Abs(x - i_0) + h)^2 + (Abs(y - j_0) + h)^2)$

End if

Set Sum ← Sum + $(B_P(x, y, k) \times D)$

End loop //y

End loop //x

Set M (k) ← sum / $(B_{Max} \times B_{Max})$

End loop

3.7.3 Cluster Number Determination

The analysis of image histogram is used to determine the number of classes (clusters) in satellite image. Ideally, the normal case supposed that each class occupy the same expansion along the colors axis. But, in actual case the classes expanded at unequal divisions depending on the appearance of the classes in the image. Therefore, to estimate the number of classes that found in the image, the standard deviation is used as a measure to quantify the amount of varying the data in the image, which leads to determine the number of classes (clusters) in that image. The following steps illustrate the way of determining the number of classes ($\boldsymbol{N_C}$) in the prepared image:

1. Determine the number of pixels in satellite image $\boldsymbol{N_T}$ by using the following relation:

$$\boldsymbol{N_T} = W * H \qquad \ldots\ldots. (3.15)$$

Where W represents the width of satellite image and H represents the height of satellite image.

2. Determine the standard deviation ($\boldsymbol{\sigma}$) to prepare image that is by employing equation (2.4) to be represented in the following form:

$$\boldsymbol{\sigma} = \sqrt{\frac{1}{N_T}\sum_{i=0}^{W-1}\sum_{j=0}^{H-1}(F_P\ (i,j) - \overline{F_P})^2} \quad \text{……. (3.16)}$$

Where $\overline{F_P}$ is the mean of the prepared image that can be computed by the following relation:

$$\overline{F_P} = \frac{1}{N_T}\sum_{i=0}^{W-1}\sum_{j=0}^{H-1} F_P(i,j) \quad \text{……. (3.17)}$$

3. Calculate the number of pixels $\boldsymbol{N}$ in the image that fall within the range of $2\boldsymbol{\sigma}$ in the image distribution.
4. Compute the percent (P) of the pixels number (N) in $2\boldsymbol{\sigma}$ expansion and the number of pixels in whole image ($\boldsymbol{N_T}$) by using the following relation:

$$P = \frac{N}{N_T} \quad \text{…….. (3.18)}$$

5. The number of classes ($\boldsymbol{N_C}$) is equal to the multiplication of the percent (P) by the maximum probable number (P_M) of classes may found in the satellite images, as follows:

$$\boldsymbol{N_C} = P * P_M \quad \text{…… (3.19)}$$

Fig (3.8) Number of cluster determination.

Algorithm: Number of cluster determination.

Input:

F_P \\ Two dimensional array represent the prepared Image.

W \\ Represent the width of image.

H \\ Represent the height of image.

Output:

$\boldsymbol{N_C}$ \\ Value represent the number of clusters in image.

Procedure:

Set Sum $\leftarrow 0$, $\overline{F_P} \leftarrow 0.0$, N$\leftarrow 0$

Set P $\leftarrow 0.0$, $P_M \leftarrow 7$

Set $N_T \leftarrow (W*H)$

Loop for *i*=0 ***to*** W

Loop for *j*= 0 ***to*** H

Set Sum $\leftarrow$ Sum $+F_P$ (i, j)

End loop //j

End loop //i

Set $\overline{F_P} \leftarrow$ Sum / (W∗H)

Set Sum $\leftarrow 0$

Loop for i=0 ***to*** W

Loop for j= 0 ***to*** H

Set Sum $\leftarrow$ Sum + $(F_P$ (i, j) $-\overline{F_P})^2$

End loop

End loop

Set SD $\leftarrow$ Sqr (Sum / (W∗H))

Loop for i=0 ***to*** W

Loop for j= 0 ***to*** H

If $((F_P$ (i, j) $\leqslant (\overline{F_P}$ + SD)) And $(F_P$ (i, j) $\geqslant (\overline{F_P}$- SD)))

Set N $\leftarrow$ N + 1

End loop //j

End loop //i

Set P $\leftarrow$ N / N_T

Set $N_C \leftarrow$ P× P_M

3.7.4 K-Means Algorithm

K-Means algorithm is an efficient unsupervised learning technique used to grouping data in terms of "*K*" clusters. These clusters are formed based on some common attribute of data. In present case, the term "*K*" represents the number of clusters (N_C), while the input data is an array of moments belongs to each image block. The K-Means is going to find out N_C of centroids that used to create dataset.

The implementation of K-Means depends on two input parameters, they are; the number of clusters (or classes) and the moment values of each block in the image. Actually, the number of classes (N_C) is estimated in the previous stage, which is used to determine the number of centroids when operating the K-means procedure. Also, the moment of each image block is computed in previous stage and stored in a moment array (*M*), which is used as an attributes of distributing the blocks on the clusters. Throughout this operation, each block is assigned an index (I_1: I_1=1, 2, 3, 4, or 5) refers to the cluster that the block belongs to. Figure (3.9) shows the main steps of K-Means algorithm, while Figure (3.10) describes the programming steps of it, in which, the function D_k ($\mathrm{M}_b, \bar{\mathrm{M}}_k$) is employed to find the Euclidean distance between two vectors for update clustering using the following relation:

$$D_k = \sqrt{\sum_{b=1}^{N} (\mathrm{M}_b - \bar{\mathrm{M}}_k)^2} \qquad \text{…….. (3.20)}$$

Where, b is index refers to the moment of the image block, and *k* is index refers to the cluster, and the function *MinIndex*(D_k) is used to find the minimum distance value from N_c distances, where k=1, 2, …, N_C.

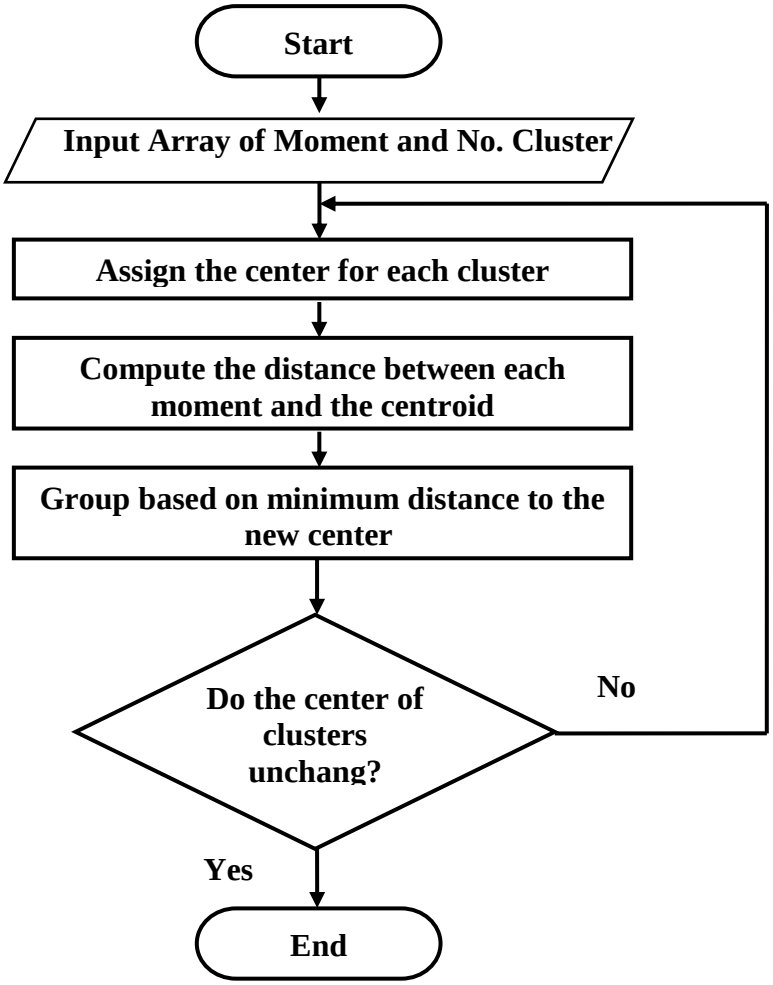

Fig (3.9) Flowchart describes the process of K-Means clustering algorithm.

Fig (3.10) Compute K-Means method.

Algorithm: Compute K-Means method

Input:

M \\ One dimensional arrays represent moment of blocks.

N_C \\ The number of clusters in prepared image.

N_B \\ number of image blocks in the image ($N_B = (W \times H)/B_{max} \times B_{max}$).

Output:

C (k_2) \\ 1D vector represents the best centroids.

Procedure:

1. Set flag ← false
2. Set C_o (k_2) randomly, k_2=1, 2…, N_C.
3. Set T ← 0
4. Do loop until flag = True OR T >= 10000.

Loop for k_1 = 0 to N_B-1

Loop for k_2 = 1 to N_C

Set D (k_1) ← Abs (M (k_1) – C (k_2))

End loop //k_2

Set I_1 (k_1) ← index of Min (D (k_1))

End loop //k_1

Set N (k_2) ← 0, S (k_2) ← 0

Loop for k_1 = 0 to N_B-1

Loop for k_2 = 1 to N_C

If I_1 (k_1) = k_2 ***then***

Set S (k_2) ← S (k_2) + M (K_1)

Set N (k_2) ← N (k_2) + 1

End if

End loop//k_2

Loop for k_2= 1 to N_C

Set C (k_2) ← S (k_2)/ N (k_2)

Set D_C ← D_C + |C (k_2) - C_o (k_2)|

```
        Set C_o (k_2) = C (k_2)
      End loop//k_2
      If D_C = 0 then
            Set flag ← true
            Set T ← T + 1
            Set C_o (k_1) ← C (k_1)
      End if
    End loop //k_1
End do loop
```

3.7.5 Dataset Formatting and Storing

This stage deals with output centroid of K-Means algorithm. The image block corresponding or closest to centroid moment is stored in two dimensional dataset array (*A*), in which each block is converted into one dimensional vector to be one column in *A*. Such that, the width of *A* is the number of classes (N_c) while the height of *A* is equal to the number of pixels found in the block (i.e., $B_{Max} \times B_{Max}$). The index I_1 is used to find the image block that corresponding to the moment centroid in each group. Figure (3.11) mentions the programming procedure of formatting and saving of dataset in the form of *A*.

Figure (3.11) Dataset (*A*) formatting and storing.

Algorithm: Dataset (*A*) formatting and storing

Input:

B_P \\ Three dimensional array represents the image blocks.

B_{Max} \\ Side length of squared image blocks (F_P).

S_i (k) \\ 1D array refer to the horizontal position of block in the image.

S_j (k) \\ 1D array refer to the vertical position of block in the image.

Output:

A \\ Two dimensional array represents the data Set that contains classes of image.

Procedure:

Set $B_L \leftarrow 0$

Set flag← false

Loop for k=0 ***to*** N_C

Loop for x=0 ***to*** B_{max}

Loop y=0 ***to*** B_{max}

Set A (B_L, k) ← B_P (x+ S_i (k), y+ S_j (k), k)

Set $B_L \leftarrow B_L$ +1

End loop//y

End loop//x ***End loop***//k

3.8 Classification Phase

The classification phase is carried out after performing the training phase. It can be achieved by two paths: block-based classification or pixel-based classification. The block-based path depends on the established dataset array *A*, where the prepared image is segmented into non-uniform blocks and then each block is assigned to the dataset array *A* to compute the classification feature. According to this feature, the block is labeled with available classes. Whereas, the

pixel-based path depends on the proximity of each pixel into the available classes in the dataset array *A*. The following subsections explain more details about the two classification paths:

3.8.1 Block based Classification

Block based classification used the SVD classification method that needs to partition the image into predefine sized image block, quadtree partitioning method is used for segmenting the image into addressed image blocks. The adopted SVD feature is estimated for each block to be compared with that of the dataset *A*. The comparison leads to classify the image blocks. More details are explained in the following subsection:

A. Image Partitioning

1. This stage needs to partition the prepared image (F_P) in non- uniform blocks using quadtree method. Figure (3.12) illustrates the algorithm of applying the quadtree partitioning method on the prepared image. The classification phase used the quadtree to segment the image into non uniform blocks restricted between B_{Max} and B_{Min}. Then each square either leaved as it or subdivided into four quadrants when it satisfies the partitioning conditions. Therefore, the implementation requires to set some parameters are related the partitioning conditions, which are used to control the process of partitioning. These control parameters are given in the following:
    1. Maximum block size ($\boldsymbol{B_{max}}$).
    2. Minimum block size ($\boldsymbol{B_{min}}$).
    3. Mean factor ($\boldsymbol{\beta}$): represents the multiplication factor; when it is multiplied by global mean ($\boldsymbol{M_g}$) it will define the value of the extended mean ($\boldsymbol{M_e}$), i.e. $\boldsymbol{M_e=\beta\times M_g}$.

4. Inclusion factor (α): represents the multiple factor, when it is multiplied by the global standard deviation (σ) it will define the value of the extended standard deviation (σ), i.e. $\sigma_e = \alpha \times \sigma$.
5. Acceptance ratio (***R***): represents the ratio of the number of pixels whose values differ from the block mean by a distance more than the expected extended standard deviation.

Fig (3.12): Image partitioning using Quadtree method.

Algorithm: Image partitioning using Quadtree method.

Input:

F_P \\ Two dimensional array represent the prepared Image.

S_i \\ 1D array refer to the horizontal position of block in the image.

S_j \\ 1D array refer to the vertical position of block in the image.

Output:

B_X \\ 1D array represents the horizontal position of the block in the image.

B_y \\ 1D array represents the vertical position of the block in the image.

B_s \\ 1D array represents the size position of the block in the image.

B_p \\ 1D array represents the pointer position of the block in the image.

B_N \\ Integer value represents number of resulted blocks.

Procedure:

Set M_g is the global mean of the image (μ)

Set S_g is the standard deviation of the image (σ)

Set Alpha is the inclusion factor

Set $S_e \leftarrow \text{Alpha} \times S_g$

Do

loop for b=1 ***to*** N_B

Set x $\leftarrow S_i(b)$

Set y $\leftarrow S_j(b)$

Set M_B is local mean of current image block.

Loop for i=0 ***to*** W-1

Loop for j=0 ***to*** H-1

If $|F_P(i,j)$ - $M_g| > S_e$ ***then***

Set $N_D \leftarrow N_D + 1$

End if

End loop //j

End loop //i

Set $R \leftarrow M_g \times N_D$ // Acceptance ratio

If $N_D > R$ ***then***

Spilt the current image block into four quadrants store postions B_x, B_y, size B_S, pointer B_p, B_N of current image block.

Get next image block

End if

Loop until there is no splitting

End loop //b

B. Feature Extraction

This stage deals with one individual block, each block resulted from the quadtree partitioning stage exported to present stage to extract its SVD feature. This is first including the conversion of the block into one dimensional vector (V) and included in the dataset array A to be the sixth column, such that the array will dimensioned as $[(N_c+1)\times(B_{Max}\times B_{Max})]$. This step is necessitated by the method of singular value decomposition (SVD) that used for classification purpose. The challenged problem is to fit the length of columns of the dataset array A with the vector V. This problem is over comes by down sampling the length of columns of A to be equal to the length of the vector V. The down sampling of each column elements is done by averaging process, in which the reducing ratio (R) is computed

by dividing the length of current image block B_L by the length of the A columns (i.e., $B_{Max}\times B_{Max}$) as follows:

$$R = \frac{B_L}{B_{Max}\times B_{Max}} \qquad \text{…….. (3.21)}$$

When the columns of the dataset array A are fitted, the *SVD* feature of current image block can be computed in comparison with dataset columns. The results are N_C values of *SVD*, each belong to one class sequentially. Figure (3.13) illustrates the algorithm of computing the *SVD* features.

Fig (3.13) SVD_s computation of image block.

Algorithm: SVD_s computation of image block.

Input:

B_P \\ Three dimensional array represents the image blocks.

A \\ Two dimensional array represents the data Set that contains classes of image with m×n dimensional (m: number of rows, n: number of columns).

Output:

SVD_k \\ 1D array represents SVD of K^{th} image block.

Procedure:

1. Down sampling the dataset A by using algorithm (a).
2. Set U← A. (This step can be omitted if A is to be overwritten with U.)
3. Set V ← $I_{n\times n}$.
4. Set $N^2\leftarrow \left(\sum_{i=1}^{n}\sum_{j=1}^{n} u_{i,j}^2\right)$, s← 0, and flag← true
5. Repeat until $s^{1/2} \leq \varepsilon\, 2N^2$ and flag = false.
   a. Set s = 0 and flag = false.
   b. For i = 1 to n − 1.
      i. For j = i + 1 to n
      - Set s ← s +$(\sum_{k=1}^{m} u_{k,i}u_{k,j})^2$.

- Determine d1, d2, by using equation (2.11).
- Set U ← $UR_{i,j}(c, s)$ where $R_{i,j}(c, s)$ is the Givens rotation matrix that acts on columns i and j during right multiplication.
- Set V ← $VRi_{,j}(c, s)$.

End loop
End loop

6. For i=1 to n

a. Compute the singular value $\boldsymbol{\sigma_I}$ by equation (2.12) .

b. Set U← US^{-1}.

End loop

7. Set SVD(k) ← S

Algorithm (a) Down sampling the Data Set (*A*).

Input:

B \\ Structured 1D array represents the fin information of each block resulted from quadtree.

A \\ Two dimensional array represents the data Set that contains classes of image.

Output:

A_d \\2D array represents the down sampling the dataset *A* with the same length of block.

Procedure:

Set R ← B_L / (B_{max}×B_{max})

Loop for $k_1 = 1$ ***to*** N_C

Set s ← 0

Loop for $k_2 = 1$ ***to*** (B_{max}×B_{max}) ***step*** (1/R)

Set $A_d(s, k_1)$ ← $A(k_2, k_1) + A(k_2+1, k_1) / 2$

Set s ← 0

End loop// k_2 ***End loop//*** k_1

C. Similarity Measurement

The differences between the computed SVD are used to compute the similarity measure (S_{V_K}) for the last column with that of its previous columns as follows:

$$S_{V_K} = 1 - \left|SVD_{N_{c+1}} - SVD_i\right| \quad \text{…….. (3.22)}$$

Where, SVD_i is the computed singular value decomposition feature of the kth class, and $SVD_{N_{c+1}}$ is the singular value decomposition of the image block that need to be classified. The maximum value of S_{V_K} refers to the class that image block is belonging to. Figure (3.14) illustrates the algorithm of assigning a class index (I_2) for each input image block.

Fig (3.14) Similarity measure Computation.

Algorithm: Similarity measure Computation.

Input:

SVD_k \\ 1D array represents SVD of Kth image block.

Output:

I_2\\ 1D array represents indices refer to any class that the block belongs to it's.

Procedure:

Loop for k=1 ***to*** N_B

Loop for i=1 ***to*** N_C

Set S_V (i) ← 1 - | SVD_k (N_C+1) - SVD_k (i)|

End loop //i

Set I_2 (k) ← index of Max (S_V) ***End loop***//k

D. Image Block Classification

When similarity measurement procedure is applied on all the image blocks, a specific color is now needed for coloring each block according to its class index

(I_2). Also, there is a color legend should be fixed to explain the meaning of colors appear in the classification results. Figure (3.15) used to describe the classification of image blocks.

Fig (3.15) Coloring each block according to its ownership to any class (According to I_2).

Algorithm: Coloring each block

Input:

B_{Max} \\ Side length of squared image blocks (F_P).

S_i \\ 1D array refer to the horizontal portion of block in the image.

S_j \\ 1D array refer to the vertical portion of block in the image.

Output:

F_C \\ Display the image result in a specific color according to the I_2.

Procedure:

Loop for k=1 ***to*** N_B

Set i ← S_i (k)

Set j ← Sj (k)

Loop for x=i *to* i+ B_{max}

Loop for y=j *to* j+ B_{max}

Set $F_C(i,j)$ ← Set_Color(I_2(k)) ***End loop End loop End loop //y, x, k***

3.8.2 Pixel Based Classification

Pixel based classification is an additional method used to classify satellite image depending on the dataset array *A*. The mean of each column of *A* is computed as follows:

$$\bar{a}_k = \frac{1}{N}\sum_{n=0}^{N} A(n,k) \qquad \text{…….. (3.23)}$$

Where, *N* represents the length of each column of *A*. The result is N_c values of means $\bar{a}$, each belong to a specific class. The classification can be done by

computing the similarity measure (S_{m_K}) between each pixel in the prepared image $F_P(i,j)$ and the means $\bar{a}_k$ as given in equation (3.24), the maximum distance refers to the index (I_3) that used to determine the color of k[th] class of current pixel. Figure (3.16) illustrates the algorithm of pixel-based classification method.

$$S_{m_K} = 1 - |\bar{a}_k - F_P(i,j)| \quad \ldots\ldots\ldots \quad (3.24)$$

Figure (3.16) Pixel Based Classification.

Algorithm: Pixel Based Classification.

Input:

a \\ 1D vector represent the mean of each column of *A* (best centroids).

W \\ Represent the width of image.

H \\ Represent the height of image.

N_C \\ Value represent the number of clusters in image.

F_p \\ represent the prepared satellite Image.

Output:

F_C \\ Display the image result in a specific color according to the minimum distance.

Procedure:

Loop i=0 ***to*** W

Loop j= *0* ***to*** H

Loop k= *0* ***to*** N_C

Set $S_m(k) \leftarrow$ 1- (*a (k)* -F_p (i, j))

End loop*//k*

Set $d_{max} \leftarrow$Max ($S_m(k)$), Set $I_3 \leftarrow$color_index (d_{max})

F_C (*i, j*) ←Set color (I_3)

End loop End loop //j,i

CHPTER FOUR

RESULTS AND ANALYSIS

CHPTER FOUR

RESULTS AND ANALYSIS

4.1 Introduction

The development of satellite imagery system brings about an easy way to extract useful information of landcover. Consequently, the behavioral performance of satellite imagery data analysis is examined using validation and assurance techniques. In the present work, there are two considered paths; enrollment and classification. The enrollment phase is useful to indicate the number of classes in the image, and then collect their features by using moment method with the K-Means algorithm to select the best classes, while the classification uses the collected classes to produce the final classification in terms of training results, also classification phase goes in two considered paths; the block oriented classification (SVD method) and the pixel oriented classification (Moment method). Result analysis is then carried out for validation purpose. The analysis includes a presentation about how algorithms are implemented mentioned in the previous chapter. Also, there is a detailed explanation related to the results achieves through implementing each stage of the proposed classification methods. The results are presented in figures and tables including the final percentage of the classification result. Then the quantitative and qualitative analysis is estimated to evaluate the performance of the proposed classification method. Moreover, the implementation of the proposed method was implemented using C# programming language, which is executed under Windows 7 operating system of 32-bit type. The dedicate classification includes interface displaying the results of each stage alone. The following sections show more details about the results and analysis of the employment method.

4.2 Used Image

The multiband satellite image used in the classification was capture by Landsat satellite, it cover the area of Baghdad city in Iraq. Figure (4.1) shows the six bands of used satellite image. The characteristics of this satellite image are listed in Table (4.1). The resolution of each band is *1024x1024 pixels*, which carried acceptable range of informatic details about the image of consideration. One of the most important factors of using the Landsat Baghdad image is the different concepts of landcover appears in the image, which leads to different classes found in the image.

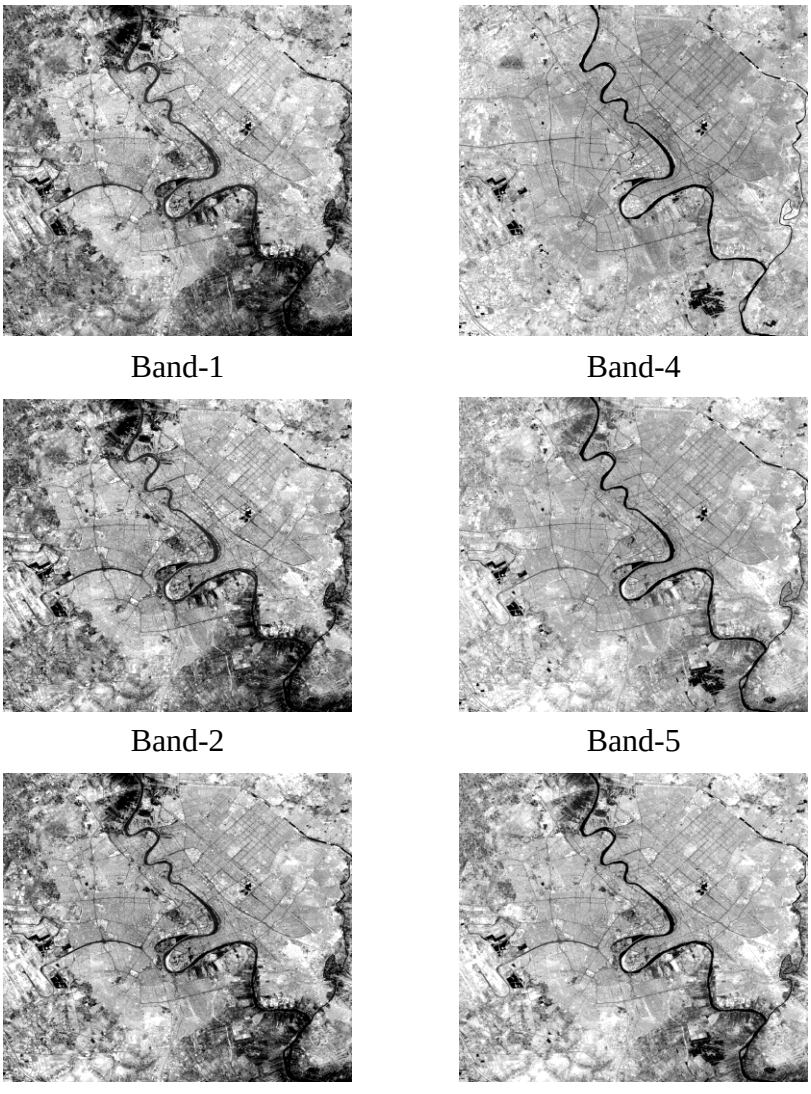

Fig (4.1) The Satellite image of Baghdad with 6-bands.

Table (4.1) Characteristics of used satellite image.

Date of capture	30/6/2015
Satellite type	Landsat- 8
Image size	1.00MB
No. of Bands	11 bands (in current consideration; the used bands are 6 only)
Spatial Resolution	30 meters
Spectral Resolution	Band1-green (0.43 - 0.45) µm Band2-red (0.45 - 0.51) µm Band3-blue (0.53 - 0.59) µm
Pixel depth	8-bit pixel values
Projection system	Universal Transformed Mercator (UTM) coordinate system and World Geodetic System 1984 (WGS84) zone 38
Image format	Geo TIFF data format
Covered area	185 kilometer (115 mile) wide swath
Sensor Type	1) Operational Land Imager (OLI) 2) Thermal Infrared Sensor (TIRS)

4.3 Image Composition Results

The results of the dispersion coefficient (*D*) of used six bands are given in Table (4.2). It is shown that the greatest three values of the dispersion coefficients are belong to the bands (1, 2, and 3) respectively. Therefore, to compose these bands with each other for making one color image, it is assumed that the band (1) is stand for green (*G*), band (2) is stand for red (*R*), and band (3) is stand for blue (*B*) in the RGB colored image. The arrangement of these bands in corresponding the color components are come from the amount of distributing the information at each color band. Figure (4.2) shows the result of the composition process. Actually, the composed image enjoyed with more contrast and more visual details.

Table (4.2) Resulted dispersion coefficient of the adopted six bands.

Band	*D*
1	0.411397722499702
2	0.402811228692944
3	0.390435892515168
4	0.259852864591293
5	0.278279684735962
6	0.319442362975303

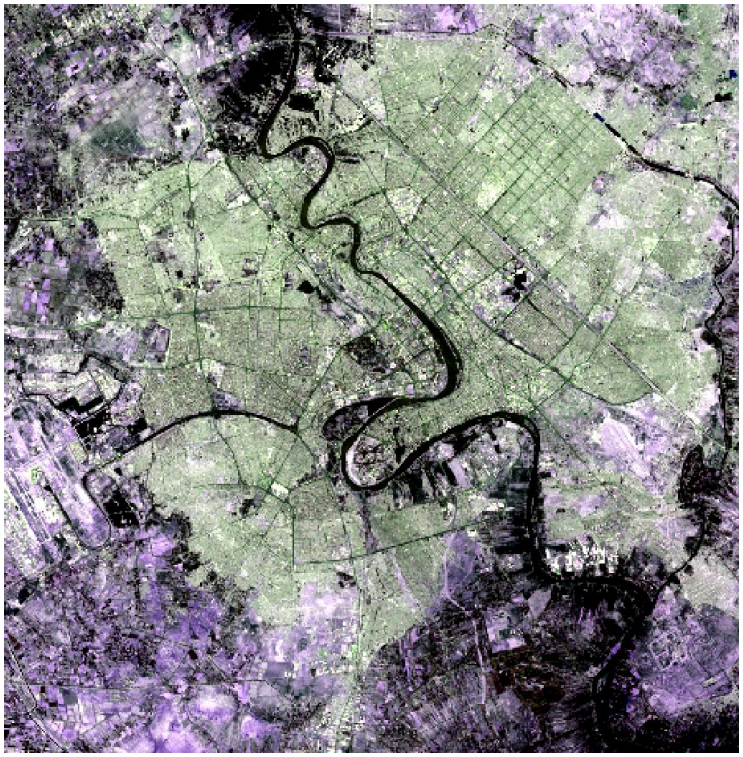

Fig (4.2) Result of the image composition.

4.4 Image Transform Result

The stage of image transform is used to enhance the satellite image by using equation (3.5). It is applied on the three color components (*R*, *G*, and *B*) of the image, which leads to converting the image from three bands into one band is better and suited for machine based analysis. Figure (4.3) shows the result of transformed image. It is noticeable that the grey image shown in Figure (4.3) has more contrast than the image composition shown in Figure (4.2). The current classification method is not sensitive to the color; such that, just the grey image is taken in to account, which has grey level variations between the image regions.

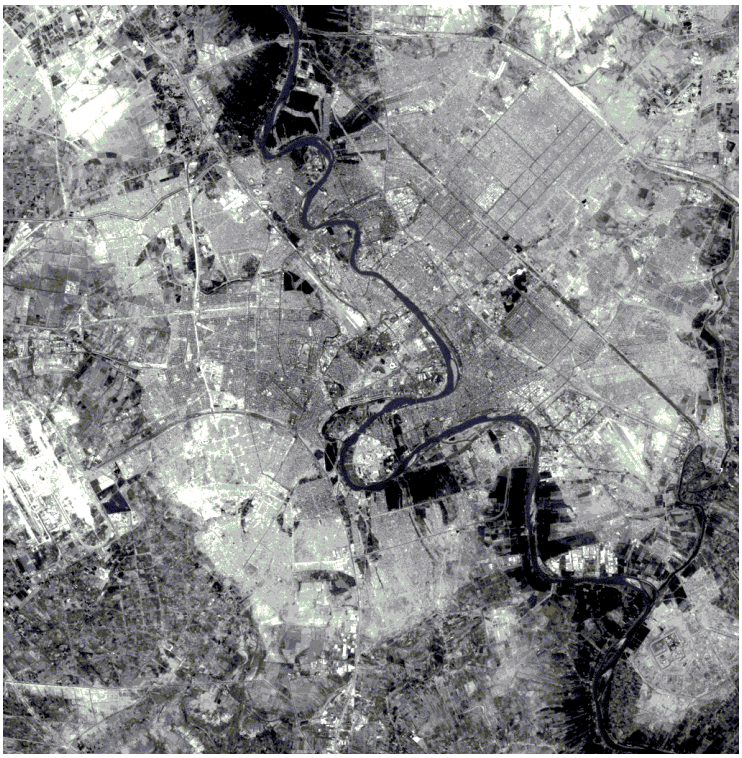

Fig (4.3) Result of image transform.

4.5 Image Preparation Result

This stage aimed to make the contrast of the considered image is full. Full contrast is achieved when choosing the values of Min_2 and Max_2 to be 0-255. The application of equation (3.6) on the transformed image gave the result shown in Figure (4.4). It is noticeable that the details of the image are clearly shown in comparison with the transformed image. Also, the color distribution in the dark region is seems to be better than that shown in the transformed image due to stretching the scale of color leads to observe few fine details in such regions. Surly, this will increase the classification score in some classes that depends on the structured details contained in the image such as resident class.

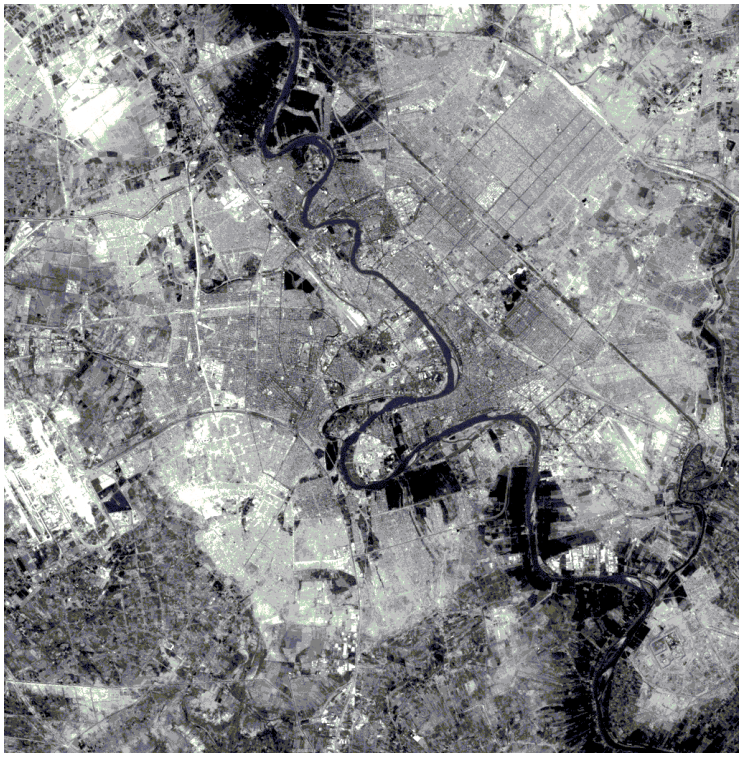

Fig (4.4) Result of image preparation.

4.6 Enrollment Phase Results

The result of enrollment phase is a dataset stored in two dimensional array (*A*), the number of columns of this array is equal to the number of classes, while the number of rows of this array is equal to the length of the class. The length of the class is equal to the number of pixels contained in the image block, which can be determined by product the width by height of the block. The following subsections explain the stages of implementing the dataset enrollment that constituting the array *A*.

4.6.1 Uniform Image Partitioning

The medium resolution of material images used in the present work make the proper values of the block size (block dimensional length) are between the range 2-8 pixels. Such that, it is set the minimum block size B_{Min} is equal to 2 *pixels* and the maximum block size B_{Max} is equal to 8 *pixels*, these values are come from a number of tries for achieving best results. Due to the uniform partitioning necessitate

partition the image into squared image blocks of size equal to B_{Max}, the results of the uniform image partitioning is shown in Figure (4.5), in which the prepared image of resolution 1024×1024 *pixel* is partitioned into image blocks each of size 8×8 *pixel*. The blocks greater than B_{Max} lead to confuse the classification results, whereas the blocks less than B_{Min} lead to poor image parts and no information may found in image blocks.

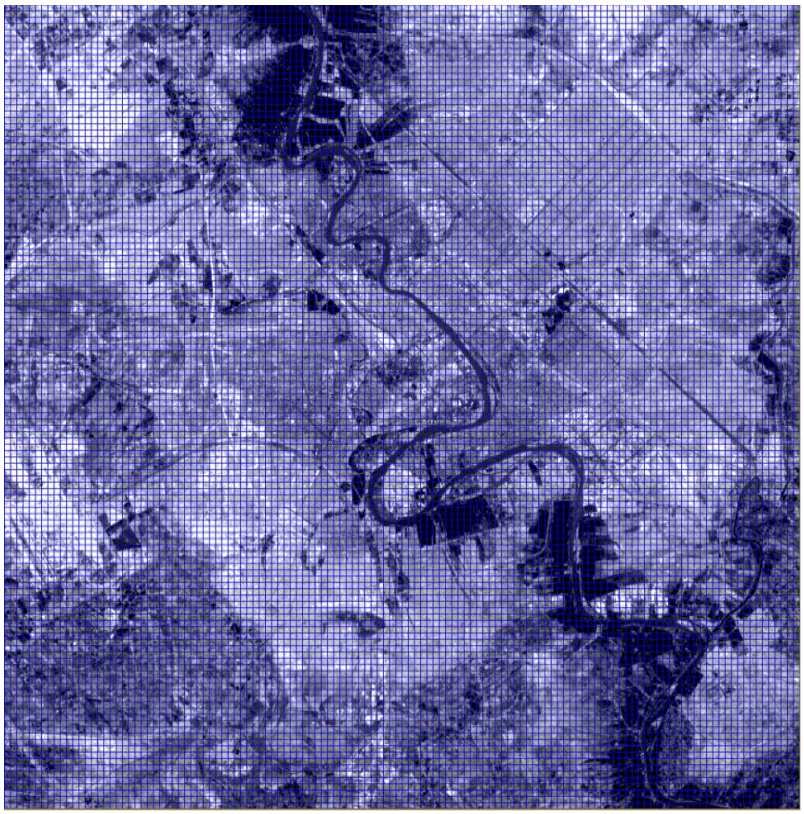

Fig (4.5) Result of uniform image partitioning (B_{Max}=8 *pixels*).

4.6.2 Moment Results

The first order moment of each image block was computed according to equation (3.14), the minimum and maximum resulted values of computed moment are shown in Figure (4.6). It is noticeable that the minimum value of the moment is zero, while the maximum value is 808.9465. The zero value refers to empty blocks, which have no information in, while the maximum value refers to much information found in that block.

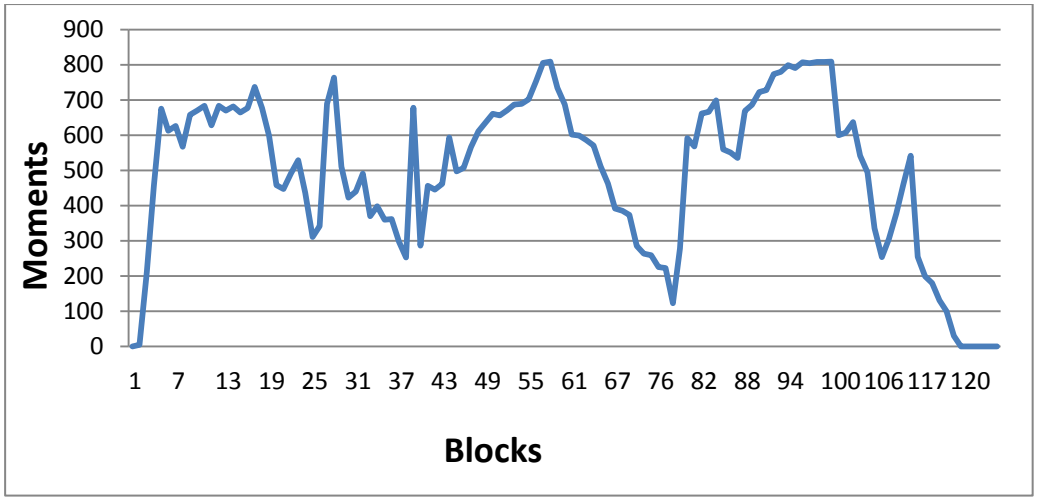

Fig (4.6) Sample range of resulted moment values.

4.6.3 Clusters Number Result

The application of algorithm (3.6) for estimating the number of classes may found in the used satellite images is lead to give the results shown in Table (4.3) when the maximum probable number of classes (P_M) is set to be 7, which showed the number of distinguished classes found in the image is five:

Table (4.3) Resulted values of algorithm (3.6) when P_M=7.

Parameter	Value
N_T	1048576
σ	60.187
$\overline{F_P}$	135.305
P	0.73087
N_c	5

4.6.4 K-Means Result

The application of the K-Means needs to set the range of expanding the clusters along the moment scale. Therefore, the range between the maximum and minimum values of the moment is 808.9465, which is divided into five (N_C=5) of

regions each of which extended by a maximum distance is equal to (D_k=808.9465/5=161.7893 *unit*). The results of the moment centroids are listed in Table (4.4). It is shown that the number of iterations needed to get convergence is 16, the low iteration values indicate the strength of the moment feature for grouping image blocks, and good choosing of distinct initial centroids. The final centroids point out the image blocks that employed to establish the dataset array *A*.

Table (4.4) K-means results of moment centroids.

Classes	Initial Centroid (Clusters)	Final Centroid (Clusters)	Number of Iteration
$Class_1$	97.073591	67.298772	16
$Class_2$	258.86291	278.5224	
$Class_3$	420.623	413.4794	
$Class_4$	582.44155	534.1971	
$Class_5$	744.231	673.69034	

4.6.5 Dataset Result

The dataset array *A* contains image blocks corresponding to the final centroids found in the third field of Table (4.4), each of these blocks represents a one column in the dataset array *A* sequentially. Figure (4.7) shows the behavior of these five columns that represent the labels of the discovered five classes of the image under consideration. Also, it is shown that the mean (μ) and variance (σ^2) of each class appear in the used image are different according to class label, whereas Figure (4.8) displays the position of the image blocks that consisting in the dataset array *A*. It is observed that dataset had contained different classes, which confirms the correct path of clustering, where the resulted classes were far away from each

other by an equivalent distances in the grey scale depending on the details of each class.

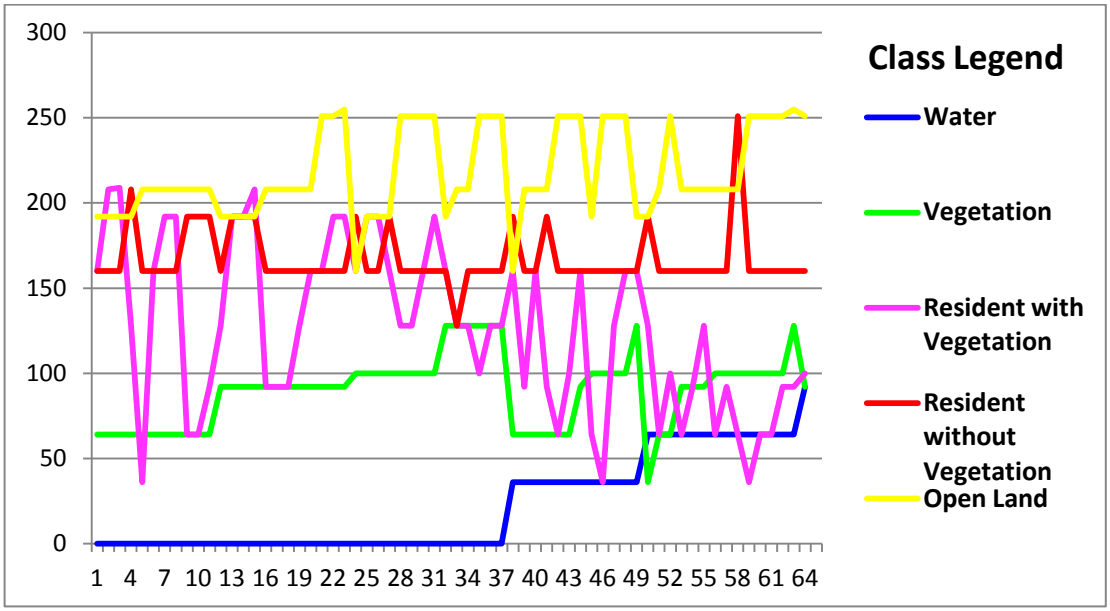

Fig (4.7) Behavior of five columns of five classes in the image.

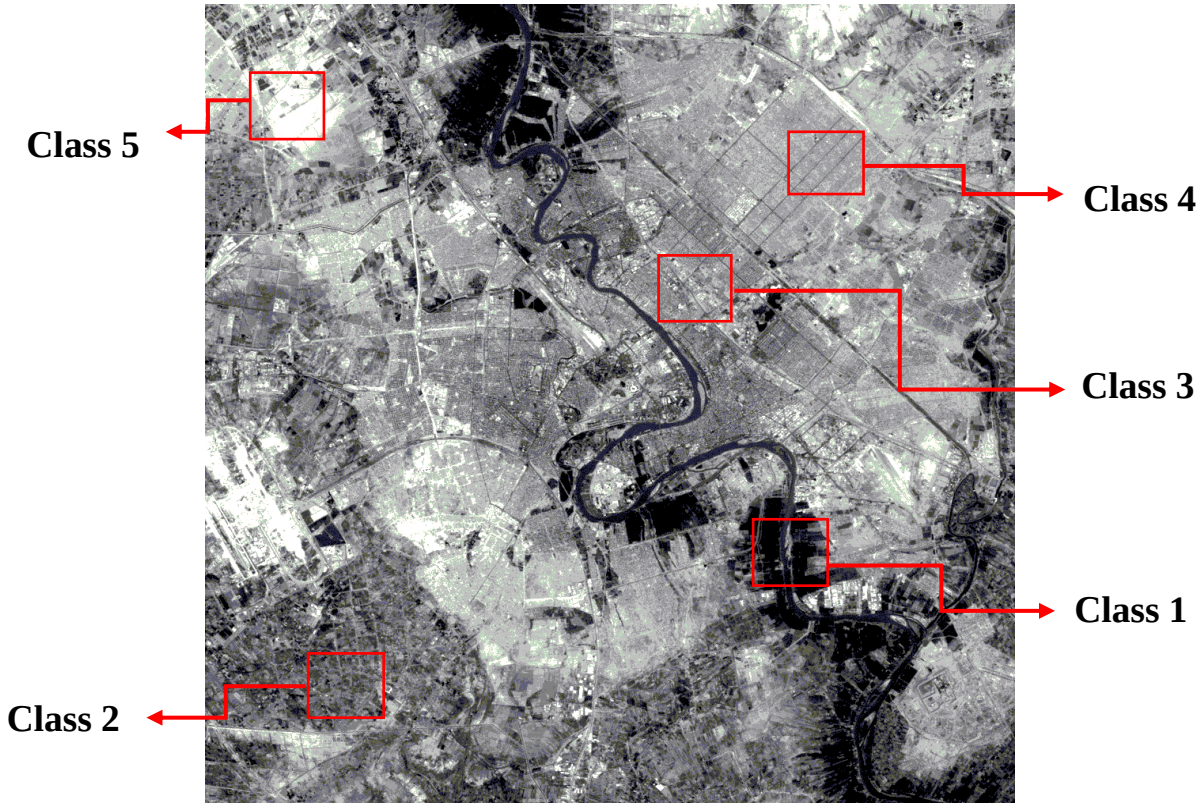

Fig (4.8) Resulted five classes.

4.7 Quadtree Partitioning Results

In the block-based classification (SVD method), the finding of best values of control parameters is very important problem since the control parameters govern the partitioning process that lead to intended classification. In order to achieve best partitioning results, the control parameters of the quadtree partitioning method were considered with the different values, Figures (4.9-4.14) illustrates the effect of the partitioning control parameters on the quadtree partitioning process. It is noticeable that the partitioning shown in Figure (4.9) is the best due to the intention of partitioning is increased at the region of fine details, while it slowly decreases at the regions of fewer details. For the used image, the best values of the control parameters that showed best partitioning results are given in Table (4.5). Such block size can shows relatively small ground details in the image of study.

Table (4.5) Best control parameter values of quadtree partitioning method.

Description	Symbol	Value
Maximum block size	B_{max}	8*pixel*
Minimum block size	B_{min}	2*pixel*
Threshold	β	0.6
Inclusion Factor	α	0.6
Acceptance ratio	R	0.2

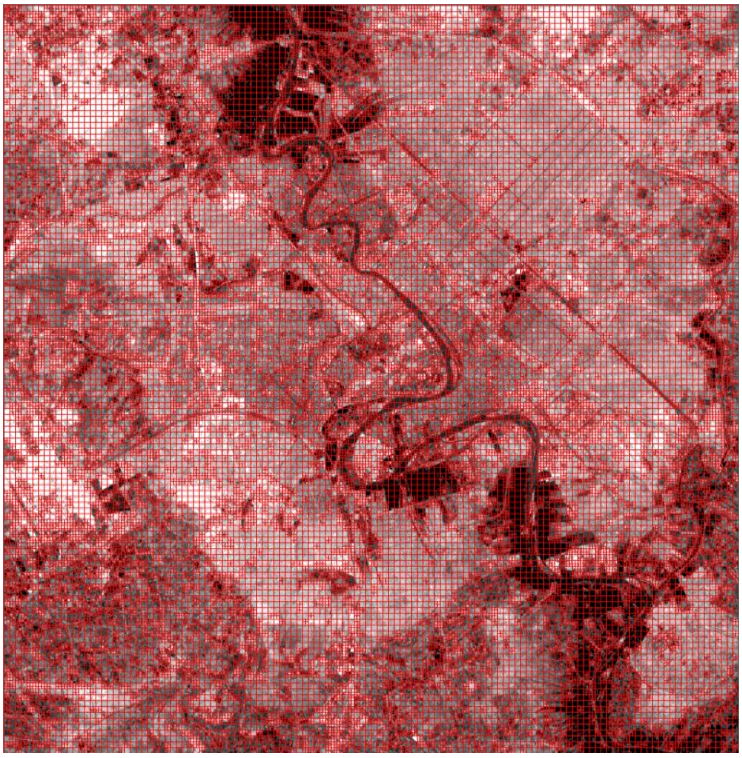

Maximum block size=8

Minimum block size=2

Acceptance ratio =0.2

Inclusion factor = 0.6

Threshold =0.6

Fig (4.9) Result of quadtree partitioning for control parameters, for B_{min}=2 and B_{max}=8.

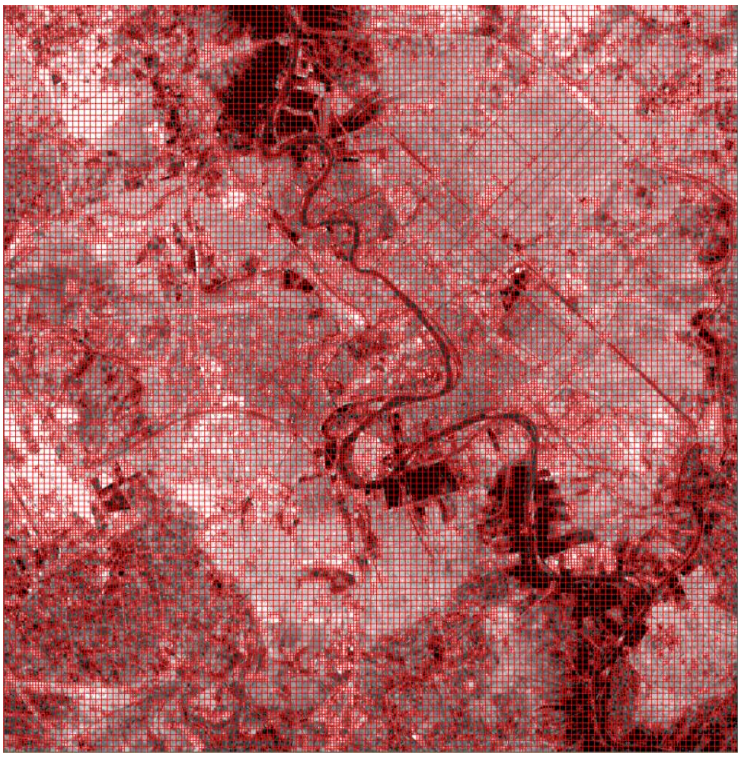

Maximum block size=8

Minimum block size=4

Acceptance ratio =0.2

Inclusion factor = 0.6

Threshold =0.6

Fig (4.10) Result of quadtree partitioning for control parameters, for B_{min}=4 and B_{max}=8.

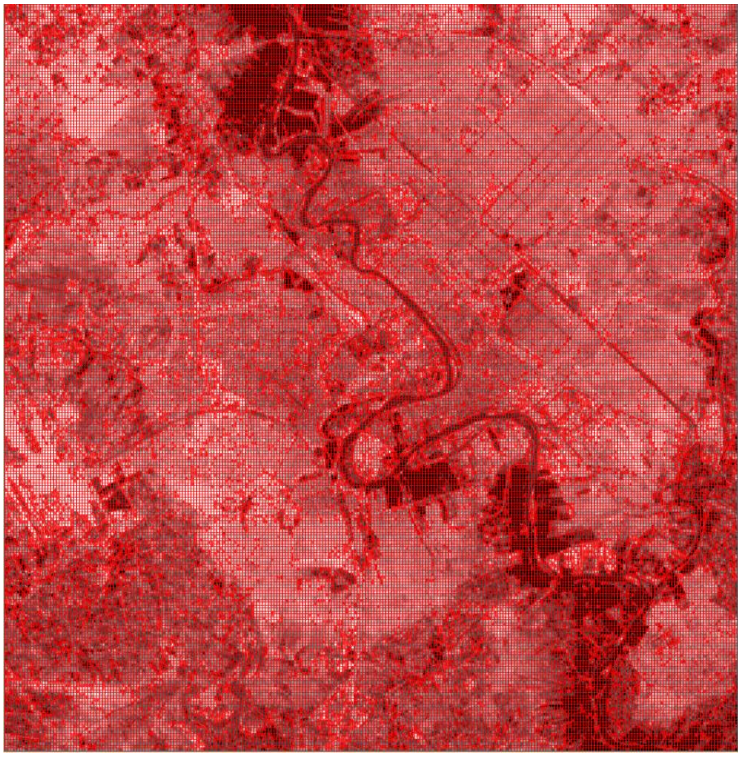

Maximum block size=4

Minimum block size=2

Acceptance ratio =0.2

Inclusion factor = 0.6

Threshold =0.6

Fig (4.11) Result of quadtree partitioning for control parameters, for B_{min}=2 and B_{max}=4.

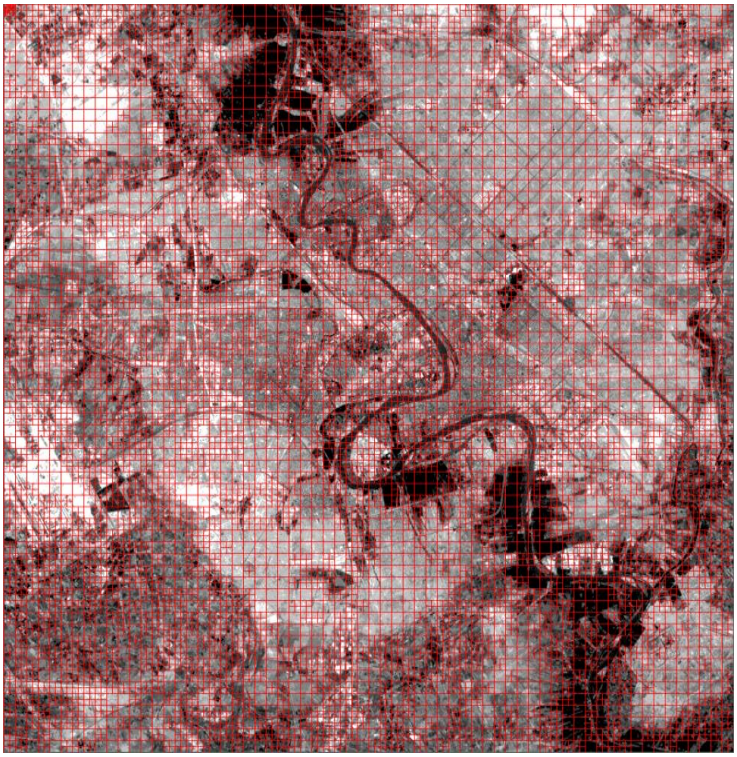

Maximum block size=16

Minimum block size=2

Acceptance ratio =0.2

Inclusion factor = 0.6

Threshold =0.6

Fig (4.12) Result of quadtree partitioning for control parameters for B_{min}=2 and B_{max}=16.

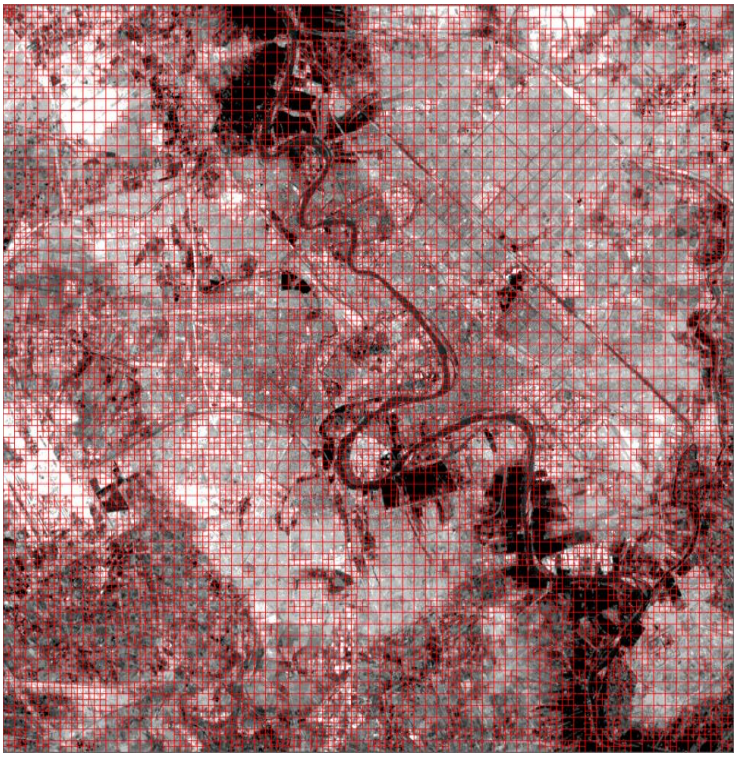

Maximum block size=16

Minimum block size=4

Acceptance ratio =0.2

Inclusion factor = 0.6

Threshold =0.6

Fig (4.13) Result of quadtree partitioning for control parameters for B_{min}=4 and B_{max}=16.

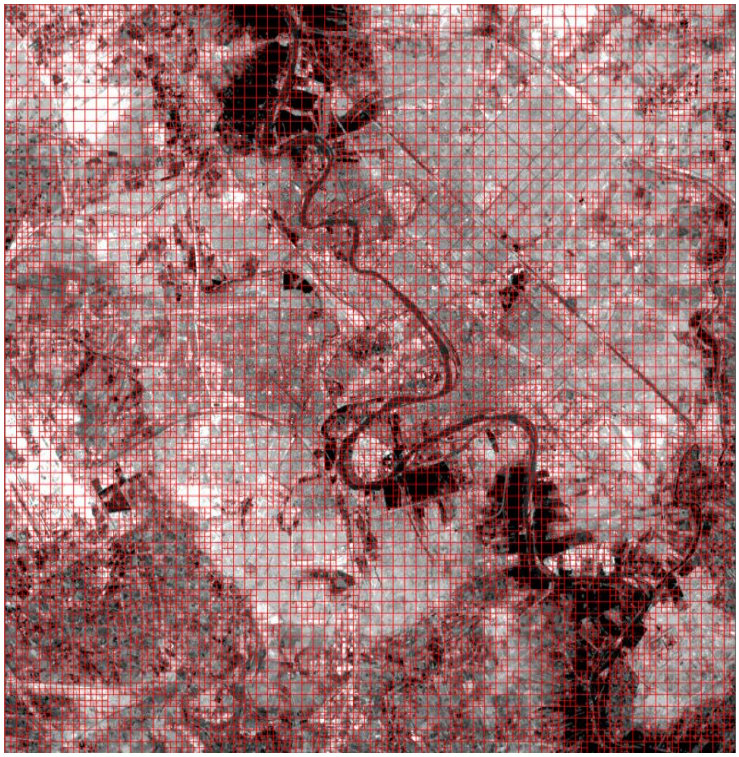

Maximum block size=16

Minimum block size=8

Acceptance ratio =0.2

Inclusion factor = 0.6

Threshold =0.6

Fig (4.14) Result of quadtree partitioning for control parameters, for B_{min}=8 and B_{max}=16.

4.8 Classification Results

Figure (4.15) displays the classification result of the prepared image using the SVD method (block-based classification). It is shown that the distribution of classes along the image region was acceptable. The best values of control parameters make the partitioning process more accurate, which leads to accurate classification results. It seen that the results of image partitioning based on image homogeneity measurements are very acceptable. The result of the partitioning depends on the quantity of the uniformity for each block. Regions of uniform extended color are partitioning into large size image blocks, this is due to less image cues are appeared in such regions. While the more details regions was partitioning into less size image blocks. This behavior of image partitioning reflects the quality of the used partitioning method. On the other hand, Figure (4.16) displays the classification result of the image using moment method (pixel-based classification). The distribution of image classes along the image region is seems to be similar to that of the block-based method. Also, it is noticeable that both methods were able to sense the small variation found in some image regions, and truly classifying the fine details that regions.

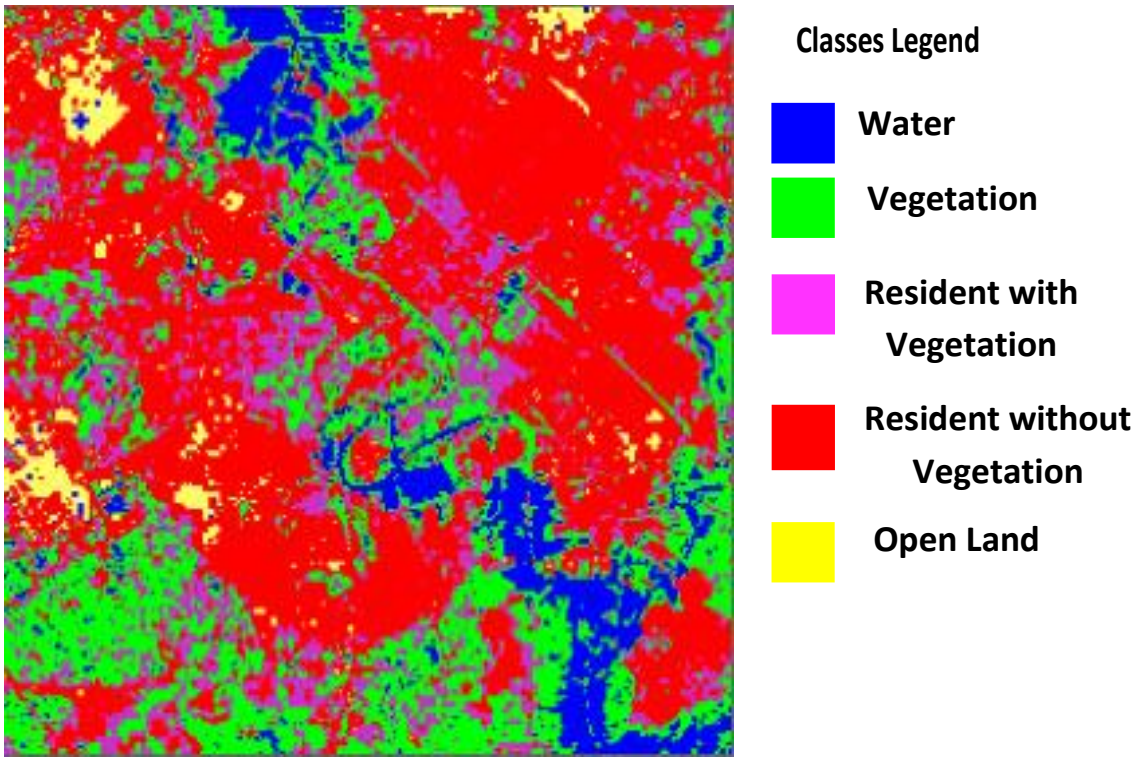

Fig (4.15) Classified image using SVD method.

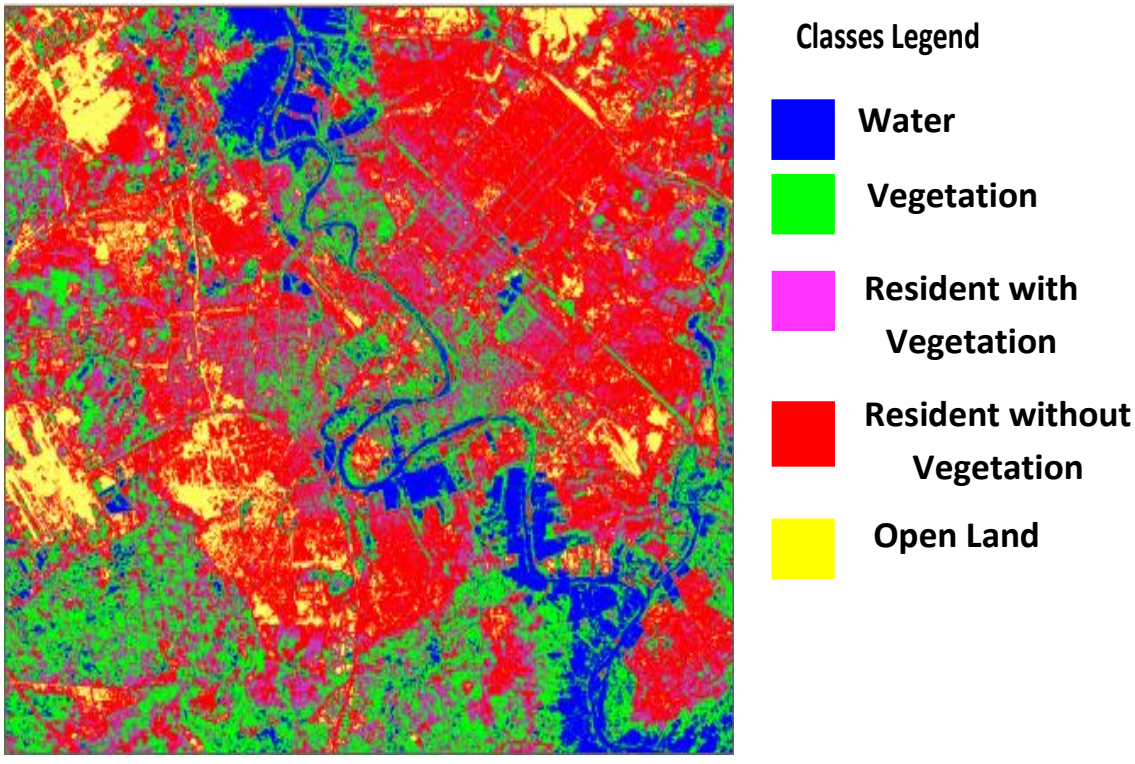

Fig (4.16) Classified image using Moment method.

4.9 Results Evaluation

To estimate the accuracy of the proposed two methods of satellite image classification, a standard image is classified by Iraq Geological Surveying Corporation (IGSC) used for purpose of comparison. This standard image is classified by Maximum Likelihood Method using ArcGIS software version 9.3. The classification map in this image is shown in Figure (4.17), there are five distinct classes; they are: water, vegetation, residential with vegetation (Resident -1), residential without vegetation (Resident -2), and open land. The classification results were compared to the actual classification information given in Figure (4.17) to evaluate the proposed classification process.

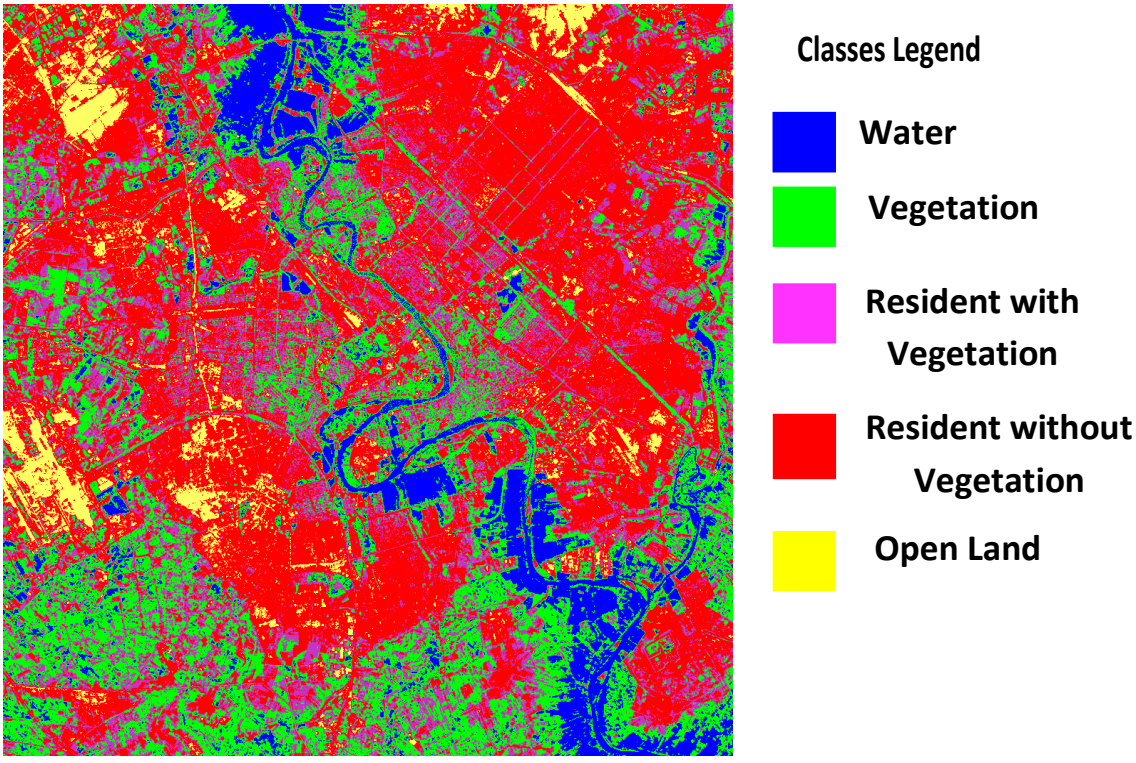

Fig (4.17) The Standard satellite image classification from IGSC.

The process of comparison was carried out pixel by pixel to guarantee the comparison result gave more realistic indication. The procedure is done by counting the number of pixels in the classified image that gave identify same class in the standard classified image. Then, the percent (P_T) of the identical classified pixels (C_p) to the total number of pixels (T_p) found in the image is computed as follows:

$$P_T = \frac{C_p}{T_p} \times 100\% \quad \ldots\ldots (4.1)$$

Where, $\boldsymbol{P_T}$ represents the overall accuracy (OA) of the proposed classification relative to the classification of the standard classified image given by GSC. Moreover, this relation can be employed to estimate the accuracy of each class in the image separately. This is carried out by examining pixels of classified image that identify same class in the standard classified image, which can be given in the following relation:

$$P_k = \frac{C_c}{C_T} \times 100\% \quad \ldots\ldots (4.2)$$

Where, P_k is the classification accuracy of k^{th} class that represents the user's accuracy (UA), $\boldsymbol{C_c}$ is the total number of pixels that classified as same as its corresponding pixels in the standard classified image given by IGSC, and $\boldsymbol{C_T}$ is the total number of pixels belong to the k^{th} class in the classified image. Accordingly, the producer accuracy (PA) can be computed using the following relation:

$$P_p = \frac{C_c}{C_p} \, x \, 100\% \quad \ldots\ldots (4.3)$$

Where, $\boldsymbol{P_p}$ represents the producer accuracy (PA), and $\boldsymbol{C_p}$ is the total number of pixels of each class in the standard classified image.

The two parameters $\boldsymbol{P_K}$ and $\boldsymbol{P_p}$ are prepared to estimate both the commission error ($\boldsymbol{E_C}$) and omission error ($\boldsymbol{E_O}$) as follows:

$$E_C = 100 - P_K \quad \ldots\ldots (4.4)$$

$$E_O = 100 - P_P \quad \ldots\ldots (4.5)$$

The use of equation (4.1) on the whole image gives best estimation for pixel classification rather than the use of random selected areas since the selection of small considered area may gave unstable result at each run of comparison due to the change of position of considered area. The evaluation results of both SVD method (block based classification) and moment method (pixel based classification) are listed in Tables (4.6 and 4.7) respectively, these tables include the overall accuracy and class accuracy for the two adopted classification methods. Further evaluation was indicated by measuring the area covered by each class using the following relations:

$$A_C = C_T \times 30 \quad \ldots\ldots (4.6)$$

$$A_s = C_P \times 30 \quad \ldots\ldots (4.7)$$

Where, A_C represent the area covered by each class in both two adopted classification methods, and A_S represent the area covered by each pixel in standard classified image. Table (4.8) shows the area covered by each class for the classified image mentioned before.

These results showed that the classification methods were successful due to the percents of identical classes (P_k) were acceptable. In SVD method, it is noticeable that the class of Resident with Vegetation (Resident -1) has less identical percent due to the details of such class is large enough to be described in the used image, while the class of water has a high identical percent due to it appeared in different spectral intensity in comparison with other classes, whereas; other classes are distributed moderately between the two mentioned classes.

In moment method, it is noticeable that the class of Open Land has less identical percent due to it appeared very bright region in the used image, while the other classes have a high identical percent. Also, the identical percent of moment method was better than that of SVD method because the later one depends on classifying the image block by block, in which the minimum block size was 2 *pixels*, which may be relatively large in comparison with the medium resolution of Landsat image. For this reason, the first order of Moment method showed better results since it was going to classify the image pixel by pixel, which independent on the image resolution.

Table (4.6) The results of SVD classification.

Classified Image	Standard Classified Image							
	Water	Vegetation	Resident -1	Resident -2	Open Land	C_T	User's Accuracy (P_K)	E_C
Water	71265	14697	554	108	1216	87840	81.13046	18.87
Vegetation	24023	161395	46607	9504	83	241612	66.79925	33.201
Resident -1	665	46725	90637	45410	259	183696	49.34076	50.659
Resident -2	136	12025	71947	392520	27776	504404	77.81857	22.182
Open Land	0.0	17	49	6053	24905	31024	80.27656	19.724
C_P	96089	234859	209794	453595	54239	1048576		
Producer Accuracy(P_p)	74.16562	68.71996	43.20286	86.53535	45.917			
E_O	25.83438	31.28004	56.79714	13.46465	54.083			
Overall Accuracy	70.64075							

Table (4.7) The results of Moment classification.

Standard Classified Image					Classified Image						
	Water	Vegetation	Resident -1	Resident -2	Open Land	C_T	User's Accuracy (P_k)	E_C			
Water	96089	0.0	0.0	0.0	0.0	96089	100	0.00			
Vegetation	0.0	234859	0.0	0.0	0.0	234859	100	0.00			
Resident -1	0.0	0.0	209794	0.0	0.0	209794	100	0.00			
Resident -2	0.0	0.0	0.0	409973	0.0	409973	100	0.00			
Open Land	0.0	0.0	0.0	43622	54239	97861	55.43	44.57			
C_P	96089	234859	209794	453595	54239	1048576					
Producer Accuracy(P_p)	100	100	100	90.38305	100						
E_O	0.00	0.00	0.00	9.61695	0.00						
Overall Accuracy	95.84										

Table (4.8) Area Covered by each pixel.

Class Name	A_S (m^2)	$A_{C_{SVD}}$ (m^2)	$A_{C_{Moment}}$ (m^2)
Water	2882670	2635200	2882670
Vegetation	7045770	7248360	7045770
Resident With Vegetation	6293820	5510880	6293820
Resident Without Vegetation	13607850	15132120	12299190
Open Land	1627170	930720	2935830

4.10 Results Analysis

The enrollment of the dataset using moment based K-Means method make the dataset is large enough, where the column length was (*64*) *Elements*. This restriction is slightly confusing the segmentation results, some segmented blocks appeared spectrally non-uniform. Thus, the use of the K-means was necessary to optimize the elements of the dataset.

Actually, the classification results mentioned in Tables (4.6 and 4.7) were acceptable since the comparison with the standard image was mostly identical. The overall accuracy of image classification was efficient and gave higher values in both methods.

The correct determination of classes' number makes the classification results to be more confident. It was observed that the true segmentation is greatly help the classifier to get each block of image to be used in SVD classification method, which absolutely leads to optimal classification results. The use of quadtree serves the classification stage due to the block size was mostly smaller time by time till reaching to spectrally homogenous region. In general, the SVD classification method and Moment classification method were successfully indicating actual

classification results to classify satellite image, which ensure the good performance of the classification and efficiency of the employment methods.

The established software showed pretty interface for displaying the output of each stage as shown in Figure (4.18). The buttons referred to principal operations that adopted in the present work.

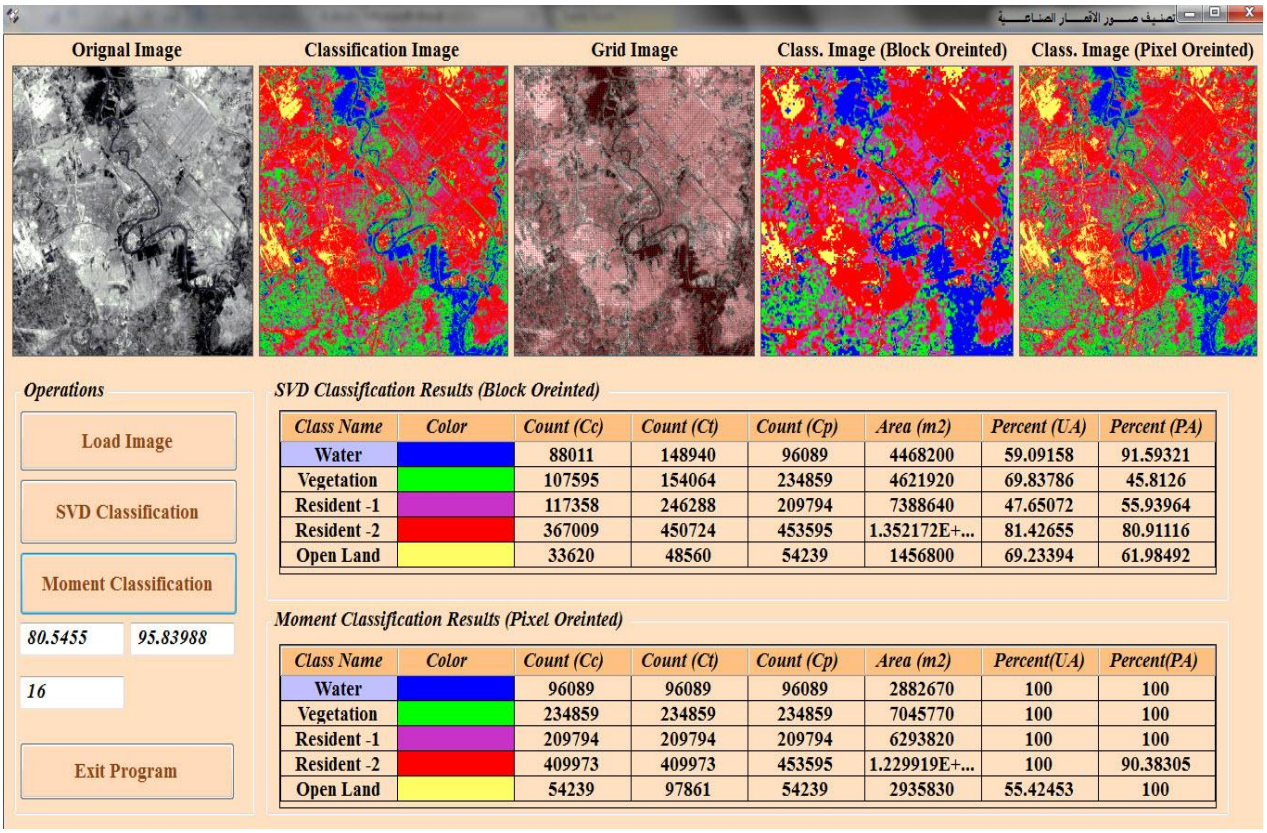

Fig (4.18) Interface of the system.

The results showed that the overall accuracy of the classified satellite image is *70.64075%*, while the total accuracy is about *81.83279%* when the Resident without Vegetation (Resident -2) and Resident with vegetation (Resident -1) classes are regarded as same class. Table (4.9), is derived from Table (4.6), in which the number of identical classes are great. The identification of classification of water class was large in comparison with other classes, this procedure is applied on other identical classes (same classes) as shown in Figure (4.19), and where the

figure gives indicates for each classified class with the percent of identical classes. Also, Figure (4.19) indicates that the class of Water showed high identification percent in comparison with that of standard image relative to other classes in the standard image.

Table (4.9) The percent of identical pixels in each class.

Class Name	Water	Vegetation	Resident With Vegetation	Resident Without Vegetation	Open Land
Water	0.7416562	0.0626	0.002641	0.0002381	0.02242
Vegetation	0.250008	0.6872	0.22216	0.020953	0.0015303
Resident With Vegetation	0.00692067	0.199	0.4321	0.100112	0.0047752
Resident Without Vegetation	0.0014154	0.051201	0.342942	0.865354	0.512104
Open Land	0.0	0.0000724	0.000233563	0.013345	0.4592

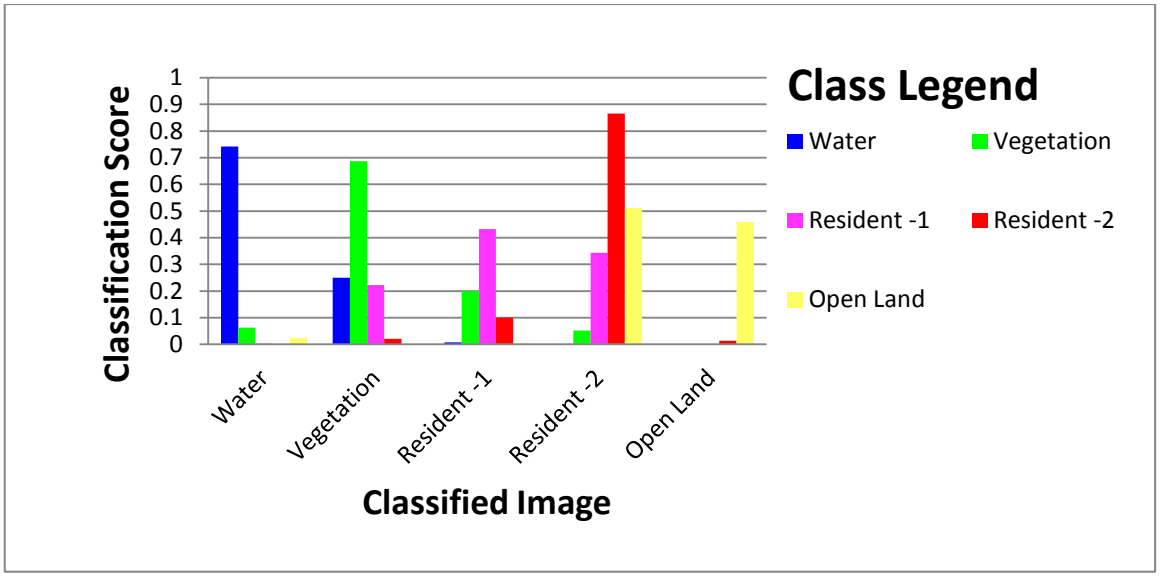

Fig (4.19) Classes accuracy in SVD method.

Moreover, Table (4.6) mentioned that the largest user's accuracy achieved with the high accuracy for the class of water, the high value of user's accuracy has been found *81.13046 %* for comparison between the results of the standard classified image and the SVD based classified image, while the smallest user's accuracy was found in the class of Resident with Vegetation *49.34067%*. It is concluded that the rest user's accuracy for the classes of satellite image are limited between the maximum and minimum percent user's accuracy. Figure (4.20) describes the user's accuracy of each class. On other hand, the high producer accuracy achieved for the class Resident without Vegetation is *86.53535%* and the smallest producer accuracy for the class Resident with Vegetation is *43.20286%* the rest classes are limited between the larger and smaller producer accuracy as shown in figure (4.21), where the class of Resident with Vegetation has the smallest accuracy value.

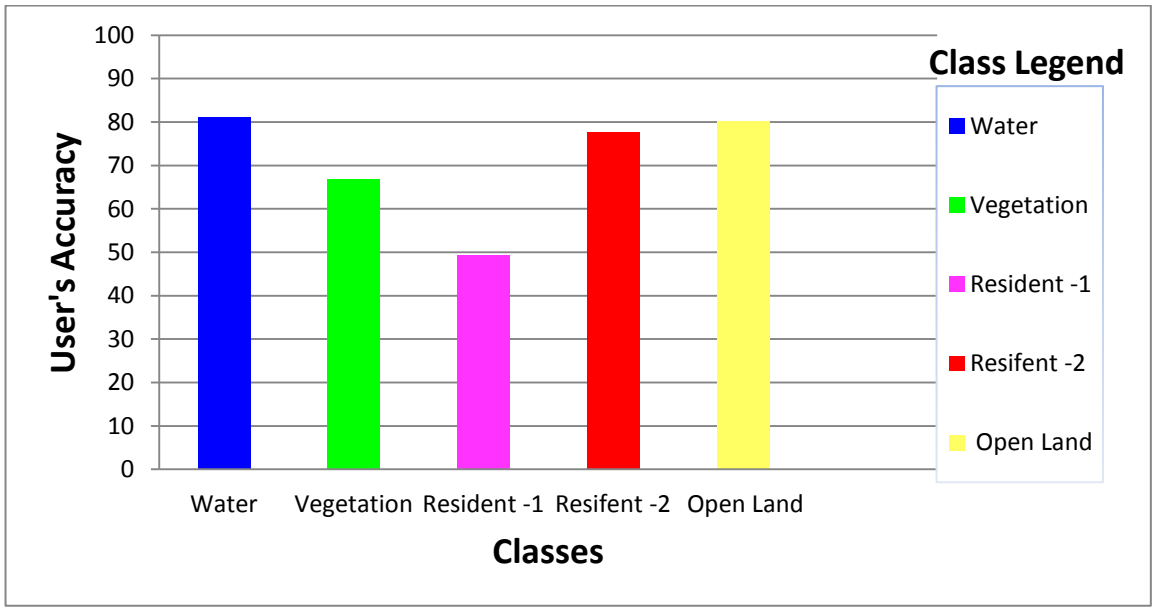

Fig (4.20) User's accuracy of classes in SVD method.

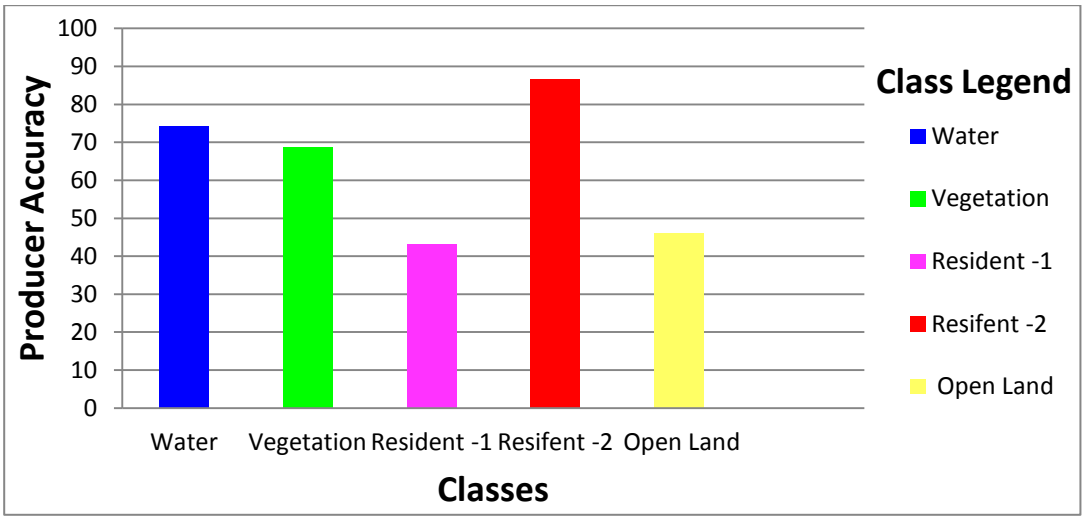

Fig (4. 21) Producer accuracy of classes in SVD method.

Also, Figure (4.22) describes the variation of each class in both user's accuracy and producer accuracy, where the user's accuracy classes: water, resident With Vegetation, and Open Land class are greater than their producer accuracy, while the user's accuracy of Vegetation and Resident Without Vegetation are less than the producer accuracy of the standard classified image, which indicates the classes of water, Resident with vegetation and, Vegetation are more changed compared with the other classes.

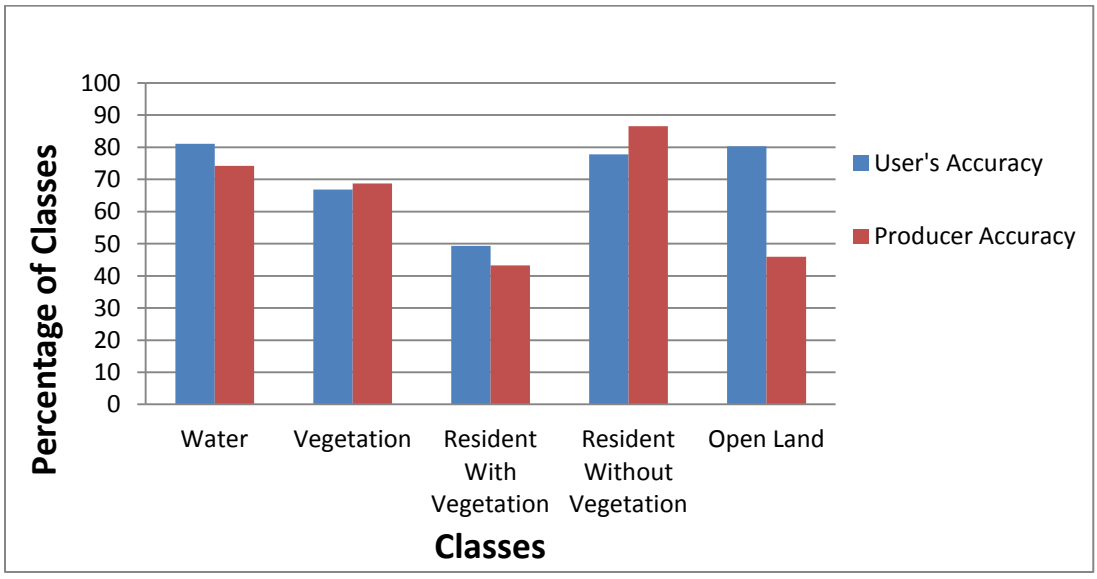

Fig (4.22) Relation between producer and user's accuracy of classes By using SVD Method.

The results of moment method listed in Table (4.7) shows that the overall accuracy of the classification is *95.84%* due to the high user's accuracy and producer accuracy are yield. This make the omission and commission errors are very small values as given in Table (4.7), the high identification percent of moment classification method are for classes: Resident without vegetation, Water, Vegetation and Resident with vegetation where the user accuracy are 100%, and user accuracy is 55.43% for class of open land, and producer accuracy of classes: Water, Vegetation, Resident with vegetation and open land are 100%, while it is 90.38305% for the class of Resident without vegetation in the standard classified image as shown in figure (4.23).

Fig (4.23) Relation between producer and user's accuracy of classes
By using Moment Method.

The user's accuracy of classes of Water, Vegetation, and Resident with vegetation of the classified image are not changed, while the producer accuracy of the standard classified image are relatively changed. The user's accuracy of the Open Land class is less than the producer accuracy. Also, the user's accuracy of the Resident without vegetation class is greater than the producer accuracy of the

standard classified image. Figure (4.24) shows the user's accuracy of each class of moment method, where the user accuracy of Open Land class is less than other classes, while the producer accuracy of Resident without vegetation class is the least as shown in figure (4.25).

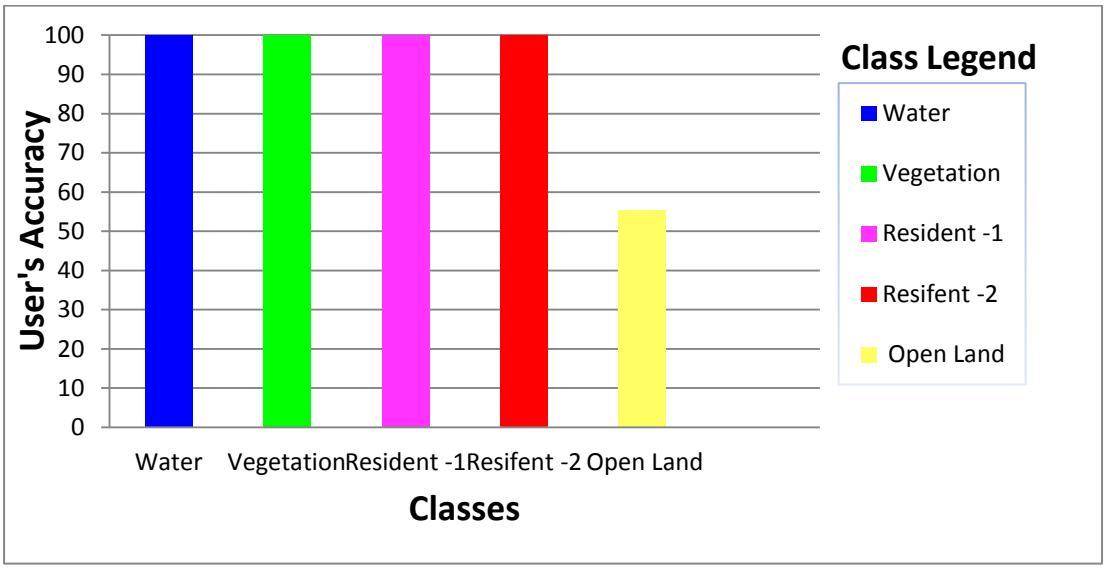

Fig (4.24) User's accuracy of classes in Moment Method.

Fig (4.25) Producer accuracy of classes in Moment method.

CHAPTER FIVE

CONCLUSIONS AND FUTURE WORK

CHAPTER FIVE
CONCLUSIONS AND FUTURE WORK

5.1 Conclusions

The most important conclusions that indicated throughout the implementation of the present work are given in the following:

1. The SVD classification method and moment method were successfully indicating actual classification results to classify satellite images.
2. The Moment classification showed high accurate classification where, the identical percent of moment classification method was better than that of SVD classification method.
3. The overall accuracy of the classified satellite image is *70.64075%*, and it is possible to be approaches 81.833% when considering both classes: residential without vegetation and residential with vegetation as one class for SVD method.
4. The classification results of SVD method show that the variation of each class in both user's accuracy and producer accuracy, where the user's accuracy classes: water, resident With Vegetation, and Open Land class are greater than their producer accuracy, while the user's accuracy of Vegetation and Resident without vegetation are less than the producer accuracy of the standard classified image, which indicates the classes of water, Resident with vegetation and, Vegetation are more changed compared with the other classes.
5. The classification results of Moment classification method show that the user's accuracy of classes: Water, Vegetation and Resident with vegetation classes are unchanged in comparison with the producer accuracy, while the user's accuracy

of Resident without vegetation is greater than the producer accuracy for about 10%. Also, the user's accuracy of Open Land class is less than that of producer accuracy for about 44.57%, which referred to the error commission.

5.2 Suggestions for Future Work

There are some suggestions taken into account for developing the implementation of the present work, which help to achieve a higher level of performance efficiency, the most important suggestions are given in the following:

1. Classify the satellite image by using Neural Network instead of Singular Value Decomposition as a block based oriented method.
2. The use of Support Vector machine beside of SVD for supervised classify satellite image with K-Means algorithm for enrollment phase that prepare Dataset *A*.
3. The use of genetic algorithm for classify satellite image beside of SVD method with K-Means algorithm for enrollment phase to prepare dataset *A*.
4. Used ISOData instead of K-Means for enrollment phase to prepare Dataset *A* with the moment of each block.
5. It can be used Fuzzy c-means instead of K-Mean for enrollment phase to prepare Dataset *A*.

REFERENCES

[Add10] Addink, E., de Jong, S. M. and Zeijlmans, M., 2010, "**Remote Sensing; a Tool for Environmental Observations**", *Utrecht University, Netherlands.*

[Akk15] Akkacha B., Abdelhafid B., and Fethi T. B., 2015, "**Multi Spectral Satellite Image Ensembles Classification Combining k-means, LVQ and SVM Classification Techniques**", *Indian Society of Remote Sensing*.

[Abu02] Al-Abudi, B. K., 2002, **"Images Data Compression using Multilevel Block Truncation coding Technique ",** *PhD. Thesis, Baghdad University, College of Science, Department of Astronomy & Space.*

[Ani11] Al-Ani L. A. and Al-Taei M. S., 2011**,"Multi-Band Image Classification Using Klt and Fractal Classifier "**, *Journal of Al-Nahrain University* Vol.14 (1), pp.171-178.

[Aqe15] Aqeel A.**A.,** 2015, **" Satellite Image Classification Using Fractal Geometry** ", M.Sc Thesis Submitted to Surveying Engineering department, College of Engineering, Baghdad University ,Iraq.

[Amm13] Ammu, A. Mathew and S. Kamatchi, April 2013, "**Brightness and Resolution Enhancement of Satellite Images using SVD and DWT",** Engineering Trends and Technology, Vol.4, P.712-718.

[Ana14] Anand, U.; Santosh, K. S. and Vipin, G.S., October 2014**" Impact of features on classification accuracy of IRS LISS-III images using artificial neural network "**, *International Journal of Application or Innovation in Engineering and Management* ,V. 3,P. 311-317.

[Ank14] Ankayarkanni and Ezil S. L., 2014, "**A Technique for Classification of High Resolution Satellite Images Using Object-Based Segmentation**", *Journal of Theoretical and Applied Information Technology*, Vol. 68, No.2, and ISSN: 1992-8645.

[Ara14] Aras, N.A., 2014," **Land Use Land Cover Classification Using Remote Sensing Techniques in Kirkuk Province", M.sc** *Thesis submitted to Physics Science department, College of Science, Baghdad University, Iraq*.

[Asw14] Aswathy M., and et al., April 2014**," Image Enhancement Using DWT DCT and SVD"***, Int. Journal of Engineering Research and Applications*, ISSN: 2248-9622, Vol. 4, Issue 4(Version 1).

[Bab14] Baboo, Capt. Dr.S S., and Thirunavukkarasu, S., May 2014,*"***Image Segmentation using High Resolution Multispectral Satellite Imagery implemented by FCM Clustering Techniques***"*, *IJCSI International Journal of Computer Science Issues*, ISSN (Print): 1694-0814 | ISSN (Online): 1694-0784, vol. 11, Issue 3, no 1.

[Bal12] Balasubramanian S. and Seldev C., 2012, **"Image Classification through integrated K- Means Algorithm",** *International Journal of Computer Science Issues,* Vol. 9, Issue 2, No 2, ISSN (Online): 1694-0814.

[Bal88] Ballanda, Kevin P.m and MacGillivray, 1988, "**Kurtosis: A Critical Review***", The American Statistician (American Statistical Association), pp.111–119.*

[Bha11] Bhandari, A. K., Kumar, A. and Padhy**,** P. K., 2011," **Enhancement of Low Contrast Satellite Images using Discrete Cosine Transform and Singular Value Decomposition",** World Academy of Science, Engineering and Technology Journal, Vol.5, P.20-26.

[Bin97] Bin, T.,Azimi-Sadjadi, M. R. Haar,T. H. V.Reinke, D., 1997, **" Neural network-based cloud classification on satellite imagery using textural features"**, *IEEE*, Vol. 3, p. 209 - 212.

[Bjo13] Bjorn F., Eric B., IreneWalde, Soren H., Christiane S., and Joachim D., 2013, **"Land Cover Classification of Satellite Images Using**

Contextual Information", *ISPRS Annals of the Photogrammetry, Remote Sensing and Spatial Information Sciences*, Volume II-3/W1.

[Bri15] Brindha S., 2015, **"Satellite Image Enhancement Using DWT – SVD and Segmentation Using MRR –MRF Model**", *Journal of Network Communications and Emerging Technologies (JNCET*), Volume 1, Issue 1.

[Bui93] Buiten, H. J. and Clevers, J. G., 1993, "**Land Observation by Remote Sensing: Theory and application**", *Gordon and Breach, Reading*.

[Chi12] Chijioke, G. E., May 2012, " **Satellite Remote Sensing Technology in Spatial Modeling Process: Technique and Procedures**", *International Journal of Science and Technology, Vol. 2, No.5, P.309-315*.

[Chr14] Chriskos P., Zoidi O., Tefas A., and Pitas I. May 2014**, "De-Identifying Facial Images Using Singular Value Decomposition"**, *Opatija, Croatia*.

[Chr13] Christopher E. N.; Segun M. O.; 3Inemesit M. A., 2013," **Supervised Learning Methods in the Mapping of Built Up Areas from Landsat-Based Satellite Imagery in art of Uyo Metropolis",** *New York Science Journal*, V.6, P.45-52.

[Dap13] Daptardar, A. and Vishal, J., 2013, "Introduction **to Remote Sensors and Image Processing and its Applications",** *International Journal of Latest Trends in Engineering and Technology*, P.107-114.

[Has07] El Hassan, I. M., 2007, **"Digital Image Processing in Remote Sensing",** *Research Center, College of Engineering, King Saud University.*

[End13] Endra O., Edwin J., Reza A., and Rinda H., 2013, **"Image Denoising by Enhancing K-SVD Algorithm",** *Internetworking Indonesia Journal***,** Vol. 5/No. 2, ISSN: 1942-9703.

[ERD13] ERDAS, Inc., 2013, **"ERDAS Field Guides",** *ERDAS Imaging, Atlanta, Georgia, USA.*

[Esh07] Eshtar, H. N., 2007, "**Multi-Temporal Analysis of Environmental Changes in Marsh Region by Landsat Images**", *M.Sc Thesis Submitted to Physics department, College of Science, AL-Nahrain University, Iraq.*

[Gon01] R. C. Gonzalez, R. E. Woods, 2001**," Digital Image Processing"**, 2nd ed., Prentice Hall, Upper Saddle River, NJ.

[Gya09] Gyanesh**,** C., Brian L. M., Dennis L. H., 2009, "**Summary of Current Radiometric Calibration Coefficients for Landsat MSS, TM, ETM+, and EO-1 ALI Sensors**", *Remote Sensing of Environment, P.893–903***.**

[Hab14] Habib M., Hadria I., and Chahira S., January 2014, "**Zernike Moments and SVM for Shape Classification in Very High Resolution Satellite Images**", *the International Arab Journal of Information Technology,* Vol. 11, No.

[Ham11] Hameed M. A. Taghreed A. H., and Amaal J. H., 2011, **" Satellite Images Unsupervised Classification Using Two Methods Fast Otsu and K-means "**, *Baghdad Science Journal,* Vol.8 (2).

[Har15] Harikrishnan.R, and S. Poongodi, March 2015, **"Satellite Image Classification Based on Fuzzy with Cellular Automata"**, *International Journal of Electronics and Communication Engineering (SSRG-IJECE),* ISSN: 2348 – 8549, volume 2 Issue 3.

[Ily13] Ilya S., James M., George D., and Geoffrey H., 2013**,**" **On the importance of initialization and momentum in deep learning"**, *International Conference on Ma-Chine Learning, Atlanta, Georgia, USA,* volume 28.

[Jay09] Jay, G., 2009, "Digital **Analysis of Remotely Sensed Imagery**", *Mc Graw Hill, New York.*

[Jia09] Jian, G. Liu and Philippa, J. Mason, 2009, "**Essential Image Processing and GIS for Remote Sensing**", *First edition, Wiley Blackwell, London*.

[Jim96] Jim, A., and Pete, S., 1996, **"Landsat 7 System Design Overview",** *IEEE, 0-7803-3068-4***.**

[Joh16] John C. Russ, 2016, **"The Image Processing Hand book ",** 7th ed., *by Taylor & Francis Group4, International Standard Book Number-13: 978-1-4987-4028-9.*

[Kag06] Kaghed, N., 2006,"**Design and Implementation of Classification System for Satellite Images based on Soft Computing Techniques***",* *Information and Communication Technologies Journal,* Vol.1, P.430-436.

[Kum12] Kumar, A**.,** Bhandari,A.K. and Padhy,P., 2012, " **Improved normalised difference vegetation index method based on discrete cosine transform and singular value decomposition for satellite image processing**", *Signal Processing, IEEE.*Vol.6,P.617-625.

[Lev99] Levin, N., 1999, "**Fundamentals of Remote Sensing** ", *International Maritime Academy, Trieste, Italy.*

[Lio94] Liou R., Azimi- Sadjadi, M.R., Reinke, D.L. and Vonder-Haar, T.H., 1994," **Detection and classification of cloud data from geostationary satellite using artificial neural networks** ", *Nural network, IEEE,* Vol. 7, p 4327 - 4332.

[Lil93] Lillesand, T.M. and Kiefer, R., 1993, "**Remote Sensing and Image Interpretation",** *Third Edition ,John Villey, New York*.

[Luk13] Luke L. and Ruben G., 2013, **"Interpolating Leaf Quad Tree Image Compression"**, *IEEE*, pp.978-1-4799-1319-0.

[Már07] Márcio L. Gonçalves1, Márcio L.A. Netto, and José A.F. Costa, 2007, **"A Three-Stage Approach Based on the Self-organizing Map for Satellite Image Classification",** *Springer-Verlag Berlin Heidelberg,* pp. 680–689.

[Mat08] Matzler, C., 2008, **"Physical Principles of Remote Sensing",** *University of Bern, Switzerland*.

[May05] Mayank T., 2005, **"Satellite Image Classification Using Neural Networks"**, *International Conference: Sciences of Electronic Technologies of Information and Telecommunications*.

[Mee14] Meenakshi K., Srinivasa Ch. R., Satya K., 2014, "**A Fast and Robust Hybrid Watermarking Scheme Based on Schur and SVD Transform",** *International Journal of Research in Engineering and Technology,* eISSN: 2319-1163, pISSN: 2321-7308, Volume: 03 Special Issue: 04.

[Nag12] Nagarajan B. and Devendran V., 2012," **Singular Value Decomposition based Features for Vehicle Classification under Cluttered Background and Mild Occlusion",** *International Conference on Communication Technology and System Design,* ISSN. 1877-7058.

[Nei04] Neil M., Lourenc M., and Herbst B. M., 2004," **Singular Value Decomposition, Eigenfaces, and 3D Reconstructions",** *Society for Industrial and Applied Mathematics,* Vol. 46, No. 3, pp. 518–545.

[Noo15] Noor Z., 2015, **" Satellite Image Classification Using Semantic Indexing Techniques**", *M.Sc Thesis Submitted to Astronomy and Space department, College of Science, Baghdad University, Iraq*.

[Par14] Parivallal, R. and Nagarajan, B., 2014," **Supervised Classification Methods For Object Identification Using Google Map Image",** International Journal of Engineering Sciences and Management Research, V. 1, P. 71-79.

[Par12] Partha S. B., and Vandana B., 2012, **"Software Fault Prediction Using QuadTree-Based K-Means Clustering Algorithm"**, *IEEE Transactions On Knowledge And Data Engineering,* VOL. 24, NO. 6.

[Pra10] Prabhakar G. V., Sajini A. P., Nithin N., 2010," **A Nonlinear Generalization of Singular Value Decomposition and Its Applications to Mathematical Modeling and Chaotic Cryptanalysis"**,*Springer Science Plus Business Media B.V.*

[Ran14] Ranjith K. J., Thomas H. A., and Mark Stamp, 2014**, "Singular value decomposition and metamorphic detection"**, *Springer-Verlag France, J Comput Virol Hack Tech*.

[Ren99] Rencz, A. N. and R.A. Ryerson, 1999, **"Manual of Remote Sensing for the Earth Sciences"**, *vol. 3, John Wiley and Sons, New York, USA.*

[Rho09] Rhonda D. P., Layne T. W., Randolph H. W., Christine E. B., 2009, **"Feature reduction using a singular value decomposition for the iterative guided spectral class rejection hybrid classifier"**, *ISPRS Journal of Photogrammetry and Remote Sensing 64* ,pp.107-116.

[Row12] Rowayda, A. S., 2012," **SVD Based Image Processing Applications: State of The Art, Contributions and Research Challenges**", *International Journal of Advanced Computer Science and Applications,* Vol.3, P.26-34.

[Sal10] Saliha A. and Slimane L., 2010**, "Indexing Binary Images using quad-tree Decomposition",** *IEEE***,** pp. 978-1-4244-6588-0**.**

[Sam11] Samiksha G., Arpita S., and Panchal V.K., 2011,"**A Hybrid Algorithm for Satellite Image Classification",** *Springer-Verlag Berlin Heidelberg*, CCIS 125, pp. 328–334.

[Sat11] Sathya, P., and Malathi, L., October 2011, **"Classification and Segmentation in Satellite Imagery Using Back Propagation Algorithm of ANN and K-Means Algorithm"**, *International Journal of Machine Learning and Computing*, vol. 1, no. 4.

[Shi13] Shivali A. K. and Vishakha V. K., 2013**," Supervised and Unsupervised Neural Network for Classification of Satellite Images ",** *International Journal of Computer Applications*, P.25-28.

[Sun15] Sunitha A., and Suresh B. G., June 2015 " **Satellite Image Classification Methods and Techniques: A Review**", *International Journal of Computer Applications*, pp. 0975 – 8887, Volume 119 – No.8.

[You13] Young G. B., You K. H., and Tae B. C., 2013 **"A Multispectral Image Segmentation Approach for Object-based Image Classification of High Resolution Satellite Imagery",** *KSCE Journal of Civil Engineering*, pp. 486-497.

Appendix (A)

Example illustrate the SVD Computation

The following steps illustrated example of the mechanism for computing singular value decomposition (SVD) for matrix A (m*n):

$$A=\begin{bmatrix}0 & 1\\ 1 & 0\\ 1 & 1\end{bmatrix}$$

Step 1. First, form $\mathbf{A^TA}$

$$A^TA=\begin{bmatrix}2 & 1\\ 1 & 2\end{bmatrix}$$

And compute its eigenvalues, λ, and (normalized) eigenvectors, v [57n]:

$$(A-\lambda I)\, v = 0$$

$$\lambda_1=3,\ V_{1=}\frac{\mathbf{1}}{\sqrt{\mathbf{2}}}\begin{bmatrix}1\\ 1\end{bmatrix}$$

$$\lambda_1=1,\ V_{2=}\frac{\mathbf{1}}{\sqrt{\mathbf{2}}}\begin{bmatrix}1\\ -1\end{bmatrix}$$

Step 2. Set

$$\sigma_{\mathbf{1}}=\|Av1\|_1=\sqrt{\lambda_1}=\sqrt{3}$$

$$\sigma_{\mathbf{2}}=\|Av2\|_2=\sqrt{\lambda_2}=\sqrt{1}$$

Step 3. Since $\sigma_1, \sigma_2 \neq 0$, we can immediately form u_1 and u_2

$$u_1=\frac{1}{\sigma_1}Av_1=\frac{1}{\sqrt{6}}\begin{bmatrix}1\\ 1\\ 2\end{bmatrix}$$

$$u_2=\frac{1}{\sigma_1}Av_2=\frac{1}{\sqrt{2}}\begin{bmatrix}-1\\ 1\\ 0\end{bmatrix}$$

The scaling ensures that both u_1 and u_2 are unit vectors. We can verify that they are orthogonal [57n]:

$$u_1^T u_2 = \frac{1}{\sqrt{12}} [1 \quad 1 \quad 2] \begin{bmatrix} -1 \\ 1 \\ 0 \end{bmatrix} = 0$$

Step 4. At this point, we have all the ingredients to build the reduced singular value decomposition [57n]:

$$A = U \Sigma V^T = \begin{bmatrix} \frac{1}{\sqrt{6}} & \frac{-1}{\sqrt{2}} \\ \frac{1}{\sqrt{6}} & \frac{1}{\sqrt{2}} \\ \frac{2}{\sqrt{6}} & 0 \end{bmatrix} \begin{bmatrix} \sqrt{3} & 0 \\ 0 & 1 \end{bmatrix} \begin{bmatrix} \frac{1}{\sqrt{2}} & \frac{1}{\sqrt{2}} \\ \frac{1}{\sqrt{2}} & \frac{-1}{\sqrt{2}} \end{bmatrix}$$

The only additional information required to build the full SVD is the unit vector u_3 that is orthogonal to u_1 and u_2 . One can and such a vector by inspection [57n]:

$$u_3 = \frac{1}{\sqrt{3}} \begin{bmatrix} 1 \\ 1 \\ -1 \end{bmatrix}$$

If you are naturally able to eyeball this orthogonal vector, there are any number of mechanical ways to compute u_3, e.g., by finding a vector u_3 $[\alpha, \beta, \gamma]^T$ = that satisfies:

Orthogonality conditions $u_1^T u_3 = u_1^T u_2 = 0$

Normalization condition $u_3^T u_3 = 1$

المُستَخلَص

أكتسبت تقنيات التحسس النائي اهتماماً واسعاً نظراً لتزايد الحاجة الى جمع البيانات حول التغيرات البيئية. حيث استخدمت عمليات تحليل الصور الرقمية لرسم خرائط الغابات وتقييم مخزوناتها، ولعبت دوراً هاماً في رصد وتقييم غطاء الارض. ان تصنيف صور الاقمار الصناعية هو نوع حديث نسبياً من التحسس النائي والذي يُستخدم فيه تصوير الاقمار الصناعية لفهم العديد من الخصائص البيئية.

ان الهدف من الرسالة هو انشاء طريقة تصنيف لصور الاقمار الصناعية بناءً على تقنية تحليل القيمة المفردة (SVD). ان طريقة التصنيف المقترحة تضم مراحل معالجة اولية للصور اضافة الى طورين من العمل هما: طور التجميع وطور التصنيف. ولكون ان الطريقة المقترحة تستخدم تقنية تحليل القيمة المفردة بأستخدام صور متعددة الحزم، تم استخدام صور مدينة بغداد في العراق مأخوذة من القمر لاندسات (Landsat) بدقة تصوير متوسطة ذات حجم 1024×1024 بكسل. يهدف طور التجميع الى استخلاص اصناف الصورة وحفظها في مجموعة بيانات (Dataset) بشكل بيانات تجريب. ولأن طريقة تحليل القيمة المفردة هي طريقة تصنيف مَرشد، فأنها لا تستطيع جمع بيانات الاصناف، ولذلك تم استخدام طريقة تفضيل المسافة (K-means) والمبنية على صفة العزم بدلاً عنها لأنشاء مجموعة البيانات. وبذلك فأن طور التجميع يبدأ بتجزئة الصورة الى اجزاء مربعة متساوية الحجم، وتم احتساب العزم لكل جزء من الصورة بأعتبارها صفة توزيع الاجزاء على اصناف الصورة. ثم أُستخدمت طريقة تفضيل المسافة لتقدير عدد تكتل بيانات الصورة ومراكزها والتي تحدد عدد الاصناف الموجودة في الصورة. تم حفظ اجزاء الصورة التي تقابل مراكز التكتلات في مجموعة البيانات لأستخدامها في طور التصنيف.

أظهر طور التجميع ان الصورة تحوي خمسة اصناف مميزة هي: ماء، خضرة، استيطان بدون خضرة، استيطان مع خضرة، وأرض مفتوحة. ولذلك تم حفظ اجزاء معينة من

الصورة في مجموعة البيانات كمناطق تدريب، حيث تم تأشير ورؤية مناطق التدريب هذه للتأكد من صحة معلومات الاصناف المتوفرة.

ان طريقة التصنيف المبنية على تحليل القيمة المفردة تتكون من عدة مراحل هي: تركيب الصورة، تحويل الصورة، تحضير الصورة، تجزئة الصورة، استخلاص الصفة، وثم التصنيف. ان تجزءة الصورة قد تمت بأستخدام طريقة الشجرة الرباعية (Quadtree)، حيث ان التجربة والتحليل قد بينا ان هناك عدة حالات ممكن ان تؤثر على عملية التجزئة والتي تم من خلالهما استنباط القيم المثلى لعوامل التجزئة التي ممكن ان تعطي افضل النتائج. ان مقياس التشابه لكل جزء من الصورة مع الاصناف في مجموعة البيانات قد اشار الى الصنف الذي ينتمي اليه جزء الصورة، وتباعاً لذلك تم تصنيف كل اجزاء الصورة.

بعد التأكد من التصرف المقبول لعملية التصنيف والتي تعتمد اساساً على معلومات مجموعة البيانات، تم تعديل مسار التصنيف ليصنف بكسلات الصورة بكسل بعد بكسل. وفي هذه الحالة تم مقارنة قيمة البكسل من الصورة بمعدل الصنف بمجموعة البيانات، حيث ان مقياس التشابه قد اشار الى نوع الصنف الذي ينتمي اليه ذلك البكسل. وطبقاً لذلك تم تصنيف جميع بكسلات الصورة بشكل جيد.

تم تقييم نتائج طريقتي التصنيف المعتمدتين بمقارنتها مع نتيجة تصنيف مرجعية تم الحصول عليها من هيئة المسح الجيولوجي العراقية (GSC). ان عملية المقارنة تمت لكل بكسل في صور نتائج التصنيف ومنها تم احتساب مقاييس التقييم، والتي اشارت الى ان عملية التصنيف قد جرت بشكل جيد نتيجةَ الى نسب التصنيف المقبولة والتي كانت بحدود ٧٠,٦٤% ومن الممكن ان تصبح نسبة التصنيف بحدود ٨١,٨٣٣ اذا اعتبرنا صنفي الاستيطان يعودان الى صنف واحد لطريقة تحليل القيمة المفردة وبحدود ٩٥,٨٤% لطريقة العزم. حيث ان هذه النتائج تشير الى قدرة الطرق المعتمدة لتصنيف صور الاقمار الصناعية ذات الحزم المتعددة. وأن هذه النتائج المشجعة قد اعطت الفرصة لتطوير العمل ليكون افضل عند استخدام صفات تصنيف ذات نتائج افضل.

جمهورية العراق
وزارة التعليم العالي والبحث العلمي
جامعة النهرين
كلية العلوم

تصنيف صور الاقمار الصناعية
بأستخدام تقنيات تحليل القيمة المفردة والفُضلى

رسالة
مقدمه الى كلية العلوم في جامعة النهرين
كجزء من متطلبات نيل درجة الماجستير
في علوم الحاسوب

من قبل

أســـد حســـين ذاري

(بكالوريوس علوم حاسبات، 2014)

اشراف

أ.م.د. محمد صاحب مهـدي الطائي

رمضان ١٤٣٧ هـ
مارس ٢٠١٦ م